# CHAPTER 4: THYMINE, URACIL AND ADENINE

## 4.1 THYMINE

Not only the pyrimidines present in the nucleic acids (cytosine, uracil and thymine) but also a great number of other pyrimidine derivatives play a vital role in many biological processes. In most biological systems vitamin B1 (derivative of 2-methyl-4-aminopyrimidine) occurs as its coenzyme, the specie that functions in biological systems [106]. Another pyrimidine alloxan was intensively studied [64,65] due to cause diabetes when administrated in laboratory animals. A number of pyrimidines derivatives are antimetabolites, been of clinical interest in cancer chemotherapy.

### 4.1.1 TAUTOMERISM AND pK VALUE

Thymine exists in two tautomeric forms the keto and the enol form, where the keto form is strongly favored in the equilibrium.

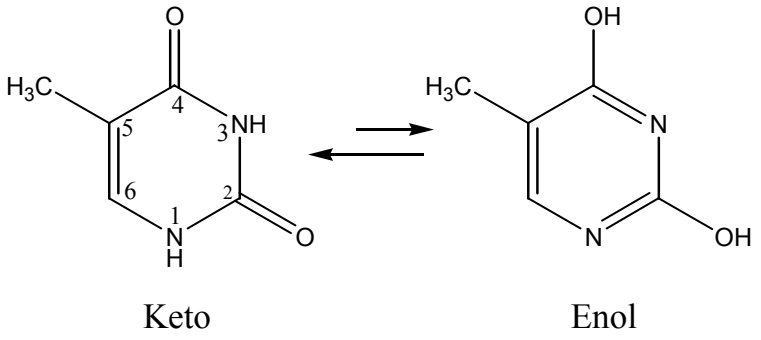


**Figure 4.1:** Tautomeric forms for thymine.

At alkaline pH the hydrogen N(3) for thymine is removed, indicating the weak basicity of the ring nitrogen.

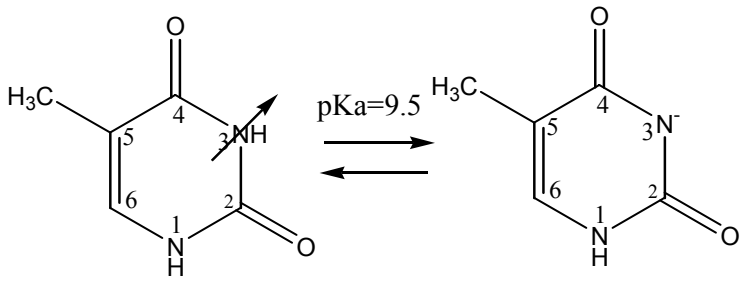


**Figure 4.2:** Ionization constant for thymine. Arrow indicates the dipole moment.

### 4.1.2 ADSORPTION OF THYMINE ON AU(111) AND AU POLYCRISTALLINE

The adsorption of pyrimidines (uracil, thymine, and cytosine) on electrode surfaces had been carefully investigated in many studies in the recent years [24,51,52,54-56]. Besides the application of these substances as corrosion inhibitors and electroplating brighteners, the DNA bases are of special interest because of their role as constituents of the nucleic acid. The use of well defined single crystal electrodes has the advantage to introduce surface sensitive techniques including STM, IR spectroscopy and x-ray to get precise information about the orientation and structure of adsorbed monolayers which in combination with chemical electrochemical methods deliver a precise view on adsorption and film formation phenomena.

It is well known that the DNA bases undergo a two-dimensional first-order phase transition on mercury and single crystal electrodes, forming well-ordered condensed monolayer.

The phase transition process depends on parameters such as bulk concentration, temperature and electrode potential [59]. Thymine represents a well-investigated system at he mercury electrode [66-69] as well as at gold single crystal electrodes [70,71]. At mercury electrodes a first order-phase transition of physisorbed thymine near the potential of zero charge (PZC) is linked to a perfect capacitive process. From electrochemical experiments we conclude that the plane of the thymine molecules in the condensed film is oriented parallel to the electrode surface. In the state of random adsorption molecules are slightly tilted with one of its nitrogen bonds towards the surface [69].

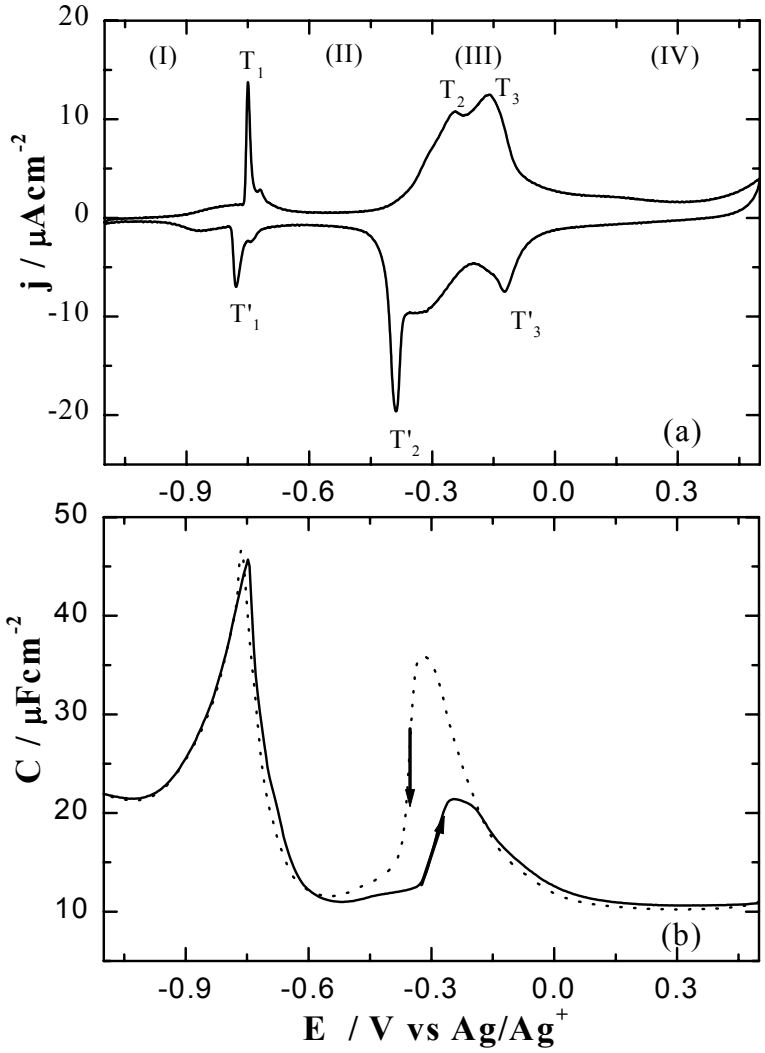


**Figure 4.3:** Cyclic voltammogram of 20 mM thymine (a) and (b) capacity curves. $T_1/T'_1$: formation and dissolution of the ordered physisorbed thymine monolayer; $T_2/T'_2$: dissolution and formation of the ordered physisorbed thymine monolayer; $T_3/T'_3$: formation and dissolution of the ordered chemisorbed thymine monolayer. Supporting electrolyte: 0.1 M $NaClO_4$ (pH = 6). Sweep rate: v = 50 mV/s (a) and v = 5 mV/s (b). Perturbation frequency and amplitude when measuring the capacity curve: 100 Hz, and 3 mV, respectively. T = 20 $^oC$.

In contrast, at gold electrodes, depending on the potential, two different well ordered adsorption layers can be recognized (Figure 4.3). At negative potentials, a first order phase transition takes place in which randomly adsorbed thymine molecules (I) form an ordered, physisorbed condensed state (II). The plane of thymine molecules is oriented nearly parallel to the electrode surface as was confirmed by STM and SNIFTIRS experiments [24,71]. In the

potential region positive of the PZC the physisorbed monolayer is transformed into a chemisorbed adsorption state of thymine (IV). This process is accompanied by, a pH-dependent, partial charge transfer from thymine to the electrode. According to in-situ STM / SNIFTIRS experiments, the plane of thymine is oriented perpendicular to the electrode surface [24,71].

Thymine molecules form stacks in this state with water molecules between the stacks [59,71]. The formation of the chemisorbed phase is a complex process, which takes place simultaneously with the lifting of the reconstruction of the surface.

In terms of capacitance (Figure 4.3 (b)), the transition between region (I) and region (II) is characterized by a relatively sharp capacity peak which indicates the increase of the surface coverage of adsorbed thymine form state I to state II. The second adsorption state (II) is marked by a nearly potential independent capacitance down to 11 $\mu Fcm^{-2}$. The transition between the states II and V is also characterized by a capacitance peak, whereby the height of the peak depends on the direction of transition. This behavior shows us that the transition form physisorbed into the chemisorbed state is significant slower than the reverse process. In the region (IV) the capacitance reaches a low and constant value, lower than the second region, which means that the thymine molecules are stronger adsorbed on the electrode surface.

Consequently, adsorption of thymine at the Au(111) electrode leads to three different adsorption states in different potential ranges: randomly adsorbed molecules (I), the physisorbed condensed monolayer (II) and the chemisorbed stacked monolayer (IV).

At higher pH values the chemisorption is less favored and, consequently, the transition process is observed at more negative potentials (Figure 4.4). Roelfs and Baumgärtel [72] demonstrated for the first time that the transition potential from physisorbed to chemisorbed phase (II to III) depends linearly on the pH. The relationship between the chemisorption and the pH dependence was explained in terms of deprotonation of the thymine molecule followed by a partial discharge in the chemisorbed state. The formed monoanions exists as a mixture of the N(1) and N(3) deprotonated forms being able to bind to the electrode surface.

Their explanation for negative changing when increasing the pH was based on the higher mobility of the protons in solution compared to the perchlorate anions. The positive/negative potentials lead to an accumulation of anions/cations near to the electrode

surface, in case of medium pH. Lowering the pH, even positive potentials are counterbalanced by elimination of protons rather than by accumulation of anions leading to an increase of the pH in the double layer compared to the bulk.

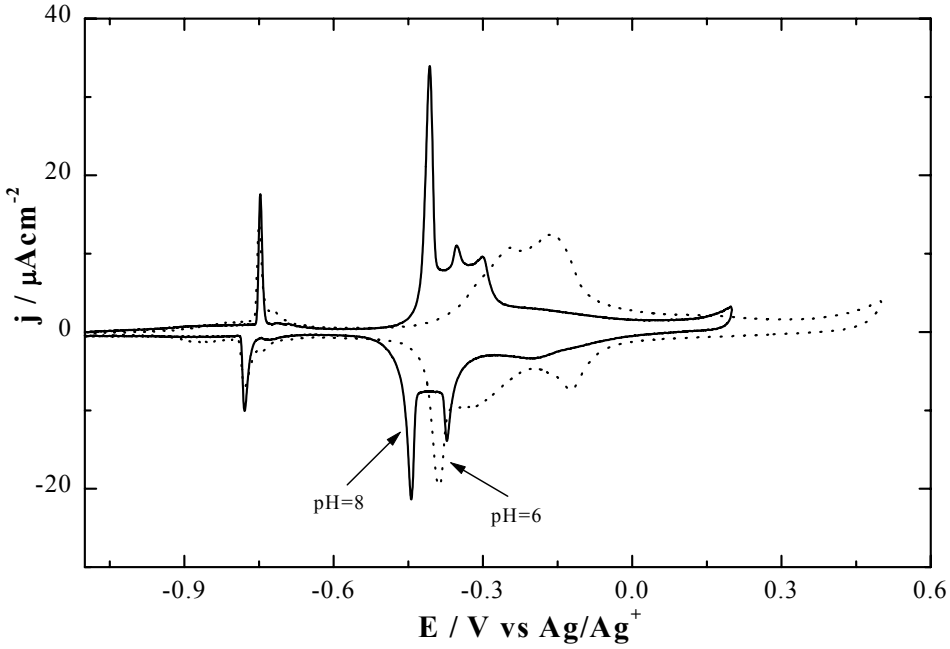


**Figure 4.4:** Cyclic voltammograms of 20 mM thymine at pH of 6 (dotted line) and 8 (full line). Supporting electrolyte: 0.1 M $NaClO_4$. Sweep rate: v = 50 mV/s. T = 20 $^oC$.

High-resolution STM images of physisorbed thymine films was investigated by Roelfs *et al.* [72] and their models fit to the ring-like structure that indeed appear to reflect the electronic density of a flat oriented thymine molecule.

The use of polarization potential map investigated by Alkorta and Perez [73] of the nucleic acid bases makes possible to elucidate the sites susceptible to nucleophilic attacks or moieties as hydrogen donors groups. According to these calculations, the N(3)H group involved in hydrogen bonds in thymine is surrounded by negative regions. Regarding to pyrimidine bases, thymine and uracil present hydrogen-bonding functions on four adjacent ring positions with two donors: N(1)H and N(3)H and two acceptors: O(2) and O(4). The formation of chemisorbed film at positive potential is linearly dependent on the electrolyte pH, which indicates that the formation of the chemisorbed film is connected with deprotonation of the adsorbed thymine molecules. The scheme of Roelfs *et al.* [72] associated

to the deprotonation explains not only the pH dependence and the charge due to formation of anionic species, but also the high stability of the chemisorbed film.

$$RNH_{solution} \longleftrightarrow RNH_{adsorbed} \quad (a)$$

$$RNH_{adsorbed} \longleftrightarrow RN^{-(1-n)}{}_{adsorbed} + H^{+}{}_{(aq)} + ne^{-} \quad (b)$$

**Figure 4.5:** Reaction scheme showing the pH dependence of chemisorbed thymine film and the charge of anionic species (After Roelfs *et al.* [72]).

This implies that thymine bonds to the electrode surface through N(1) or N(3) atom, changing its orientation from horizontal to up right position at positive potentials. In the N(1) bonded configuration one oxygen atom O(2) interact with the metal while in the N(3) configuration both oxygen atoms (O(2) and O(4)) interact with the gold electrode surface (Figure 4.6)

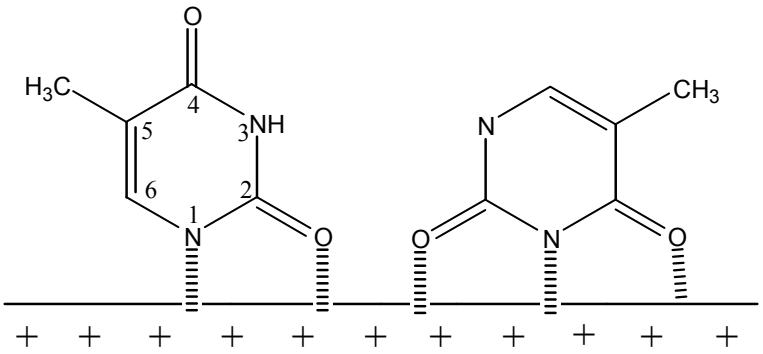


**Figure 4.6:** Two possible orientations of thymine chemisorbed on Au(111) (After Roelfs *et al.* [72]).

The adsorption of thymine on Au polycrystalline does not produce any well-solved phase-transition peaks regarding to formation and dissolution of physisorbed and chemisorbed film (Figure 4.7).

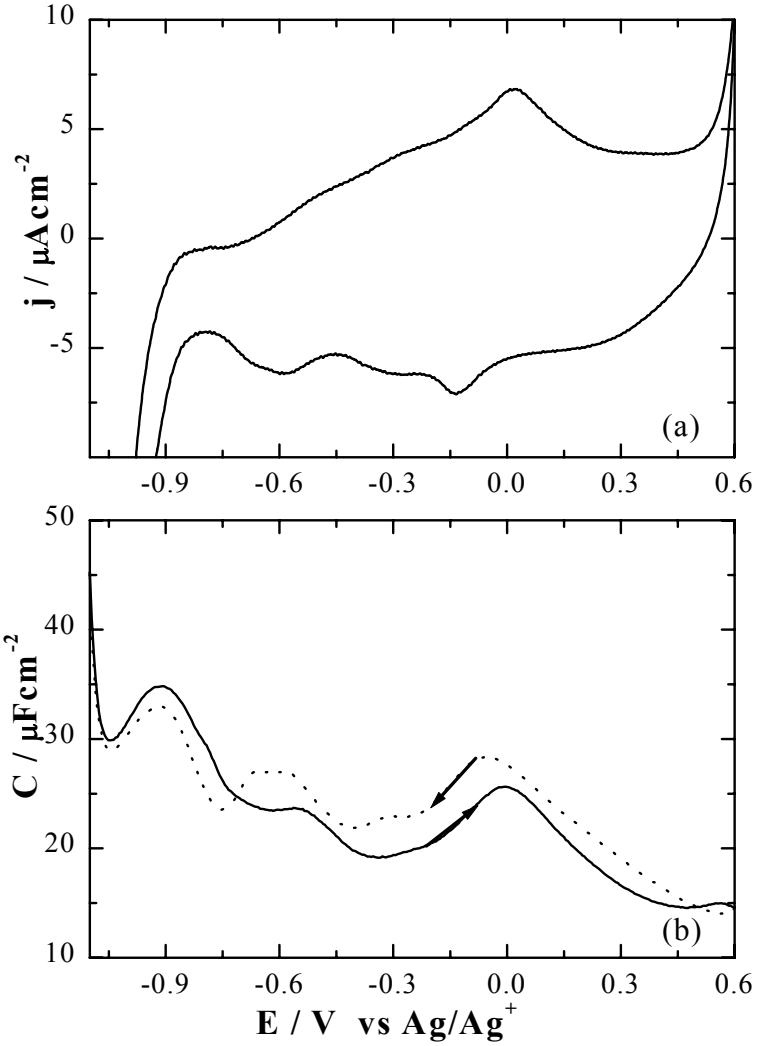


**Figure 4.7:** Cyclic voltammogram (a) and capacity curves (b) of a polycristaline gold electrode in a 20 mM thymine/0.1 M $NaClO_4$ solution. Sweep rate: v = 50 mV/s (a) and v = 5 mV/s (b). Perturbation frequency and amplitude when measuring the capacity curve: 20 Hz, and 3 mV, respectively. T = 20 $^{o}$C.

The voltammogram shows a broad wave in the positive scan. One can recognize a peak at about 0.0 V, more positive than comparable with the peaks found for Au(111) surfaces. We assign this peak to the transition between the physisorbed and chemisorbed adsorption state. Also in the negative scan it seems that the peaks shifted to more positive potentials. The electrolyte reduction starts also at more positive potentials. Also the electrolyte reduction starts at more positive potentials. The positive shifts may be an appearance of other crystal orientations than Au(111).

In the same way the peaks assigning to the phase-transition in physisorbed monolayer does not appear. We are not able to decide if a phase transition takes place. The peaks are not recognized due to the relatively high capacity current or if a phase-transition does not takes place due to the roughness of the surface, but the formation of thymine physisorbed film at negative potentials is supported by the capacitance curves (Figure 4.7 (b)).

In the forward scan (solid line) the curve minimum (18 $\mu Fcm^{-2}$) around -0.3V indicates an adsorption, whereby the peak around 0.0 V stands for a reorientation process. At positive potentials the capacitance quickly decreases, as an indication for strong adsorption (chemisorption) of thymine.

At polycrystalline electrodes two different orientation of thymine molecules are found according to the orientation found on Au(111) electrodes. Merely the kinetics of the transition differs as well as the transition potentials.

#### 4.1.2.1 KINETICS ON AU(111)

As already seen, DNA bases undergoes a two dimensional first order phase-transition on mercury and single crystal electrodes. However, only few studies considering the formation and dissolution kinetics of these adlayers have been published. Wandlowski and Dretschkow [74] performed potential step experiments to investigate the formation of uracil physisorbed film on gold single crystals, starting from a negative potential and jump to potentials inside the potential region where the physisorbed condensed film is formed. The formation mechanism is characterized by nucleation and growth processes. So far, the kinetics associated with the formation of organic films on solid electrode is more focused on uracil and some of its derivatives on gold and silver (111) and (110) surfaces [24].

On the other hand, few studies were published concerning the dissolution kinetics of the chemisorbed layer. In these studies the potential stepped was performed starting from a positive potential, where the chemisorbed layer is stable and jump in to a potential region where the physisorbed layer is formed [75]. The current-time curves were explained by a combined adsorption/desorption mechanism parallel with a two dimensional nucleation and growth process. In these studies only the dissolution of the chemisorbed phase is considered, whereby all effects regarding to condensation of physisorbed phase as well as reorientation was neglected.

#### 4.1.2.2 FORMATION OF THYMINE PHYSISORBED AND CHEMISORBED PHASE

The electrochemical way to study the kinetics of adsorption/desorption on single crystal solid electrode is to perform potential step experiments. In this section is described the investigation of the kinetics of formation and dissolution of physisorbed and chemisorbed thymine films. Figure 4.8 shows the CV of thymine and the respective current transients are shown in Figure 4.9 representing the formation of physisorbed and chemisorbed phase of thymine molecules if a potential step is applied starting from a negative potential.

Usually, the typical current vs. time transients for film formation is characterized by an initial fast exponential decaying followed by a pronounced maximum until finally the current approaches to zero. This shape implies that the process is based on a nucleation and growth mechanism. However, the transients shown in Figure 4.9 do not follow the characteristics described above. Pohlmann *et al.* [76] investigated the influence of the coupling and mutual influences of the condensation and the adsorption process in two-dimensional adsorbate systems. In their model, the maximum in the current time transients is sharper the greater is the difference between the densities of the condensed and non-condensed phases, which means that the maximum will be vanished if these two densities becomes nearly equal, a condition which is fulfilled near the critical point. This leads to the conclusion that the maximum in the current-time transients is a sufficient but not a necessary condition for two-dimensional phase transition. Additional to the coupling of adsorption and condensation, the potential step itself influences the adsorption process due to a time-dependent cell constant, RC(t).

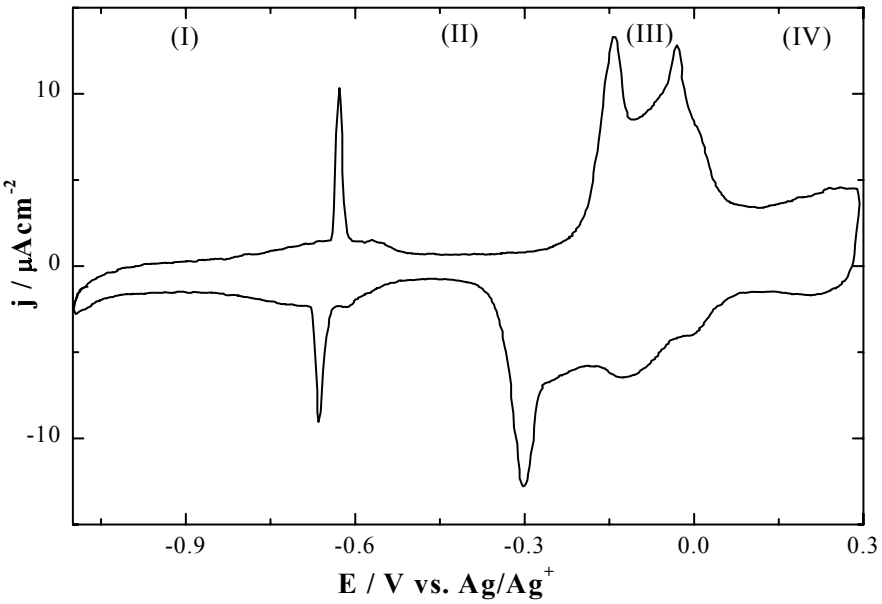


**Figure 4.8:** Cyclic voltammogram of a 14 mM thymine solution. Supporting electrolyte: 0.1 M $NaClO_4$ (pH = 6). Sweep rate: v = 50 mV/s. T = 20 $^oC$.

In the presented current vs. time curves (Figure 4.9) a maximum is well seen, but the nucleation and growth process takes place simultaneously with adsorption as well as charging of the double layer. So a detailed analysis of a nucleation and growth process could not be done. The shape of the curves is similar, independently if they reflect the formation of physisorbed or the chemisorbed layer. According to the condensation kinetics of uracil, the formation of the condensed layer becomes fast the more positive the final potential is located. In contrast, the formation of the chemisorbed phase is characterized by a fast process, showed by the first maximum followed by a slow process, which is not finished in the time region shown in Figure 4.9b. The transients do not reach the zero line. This result is in accordance with the capacity curves shown in Figure 4.3.

The closer the time constants of all participated processes (potential step, adsorption, condensation) become more are the processes coupled. Therefore a consideration of only one process or the simple adding of the different currents assigning to the processes leads to erroneous conclusions.

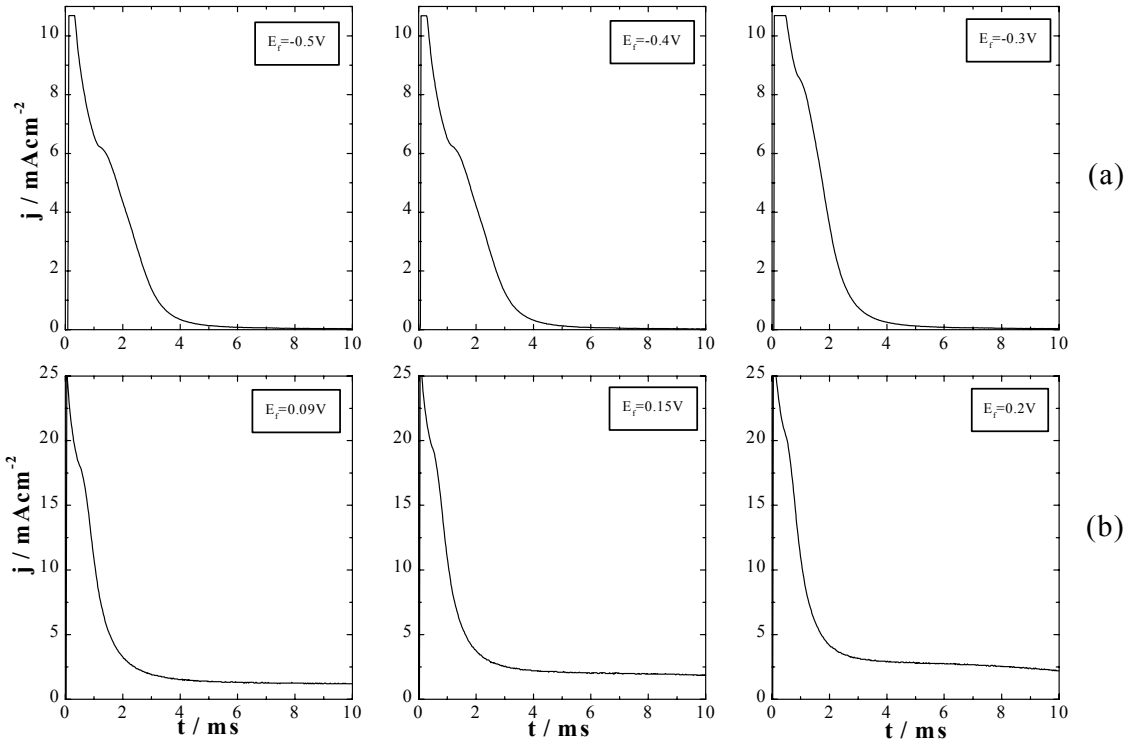


**Figure 4.9:** Current-time curves obtained after applying a single potential step from $E_i$ = -1.0 V (region I in Figure 4.8) to various final potentials into the (a) physisorbed, and (b) chemisorbed film. The waiting time at $E_i$ was 20 s. Remaining conditions identical as given in Figure 4.8: 14 mM thymine solution in 0.1 M $NaClO_4$ (pH = 6), T = 20 $^0$C.

### 4.1.2.3 DISSOLUTION OF THE PHYSISORBED AND CHEMISORBED THYMINE PHASE

In this part we deal with the dissolution kinetics of the thymine chemisorbed layer (region IV) on Au(111). The Figure 4.10 shows the transients recorded after a single potential step from $E_i$ = 0.21 V (Figure 4.8, region V) to various final potentials ($E_f$) located in region III or II, respectively. The transients stepped inside the region III (Figure 4.10 (a)) are characterized by an initial fast current decay followed by a maximum until approaches to zero. The transients become faster the more negative are the final potentials, which correspond to the higher overvoltages of the thermodynamic phase transition potential around the region III. The shape of the transients is a proof for the nucleation and growth process, as was proposed for the dissolution of uridine layers on Au(111) electrode [75]. Choosing the final potential inside the region II (Figure 4.10 (b)), one obtains more complex transients in

comparison with region III (Figure 4.10 (a)). The maximum well resolved in Figure 4.10a shifts to shorter times. Additionally, a second maximum occurs for longer times. At very negative potentials (-0.7 V) a third maximum appears in the current-time transients. The thymine molecules are characterized by forming a strong adsorbed layer at positive potentials (region IV) and the dissolution process of this film is not so simple to be understood. The thymine chemisorbed film is very stable. The electrode is completely covered by the organic film and the water molecules have no space to adsorb. Between $-0.3 < E_f < 0$V the molecules start to desorbs and undergoes a reorientation from perpendicular (region IV) to tilted orientation (region III). Simultaneously, the surface coverage decreases and the water molecules occupy the free sites between the tilted thymine molecules. Negative from $E_f = -0.3$ V (region II), the thymine molecules reorient again from tilted to planar (II) orientation. Again the surface becomes covered by an ordered condensed film "expelling" the water molecules. Dissolution of uracil chemisorbed films showed a similar behavior and the analyses by ATR-SEIRAS revealed the dissolution mechanism controlled by a hole nucleation and growth plus a Langmuir type dissolution [77].

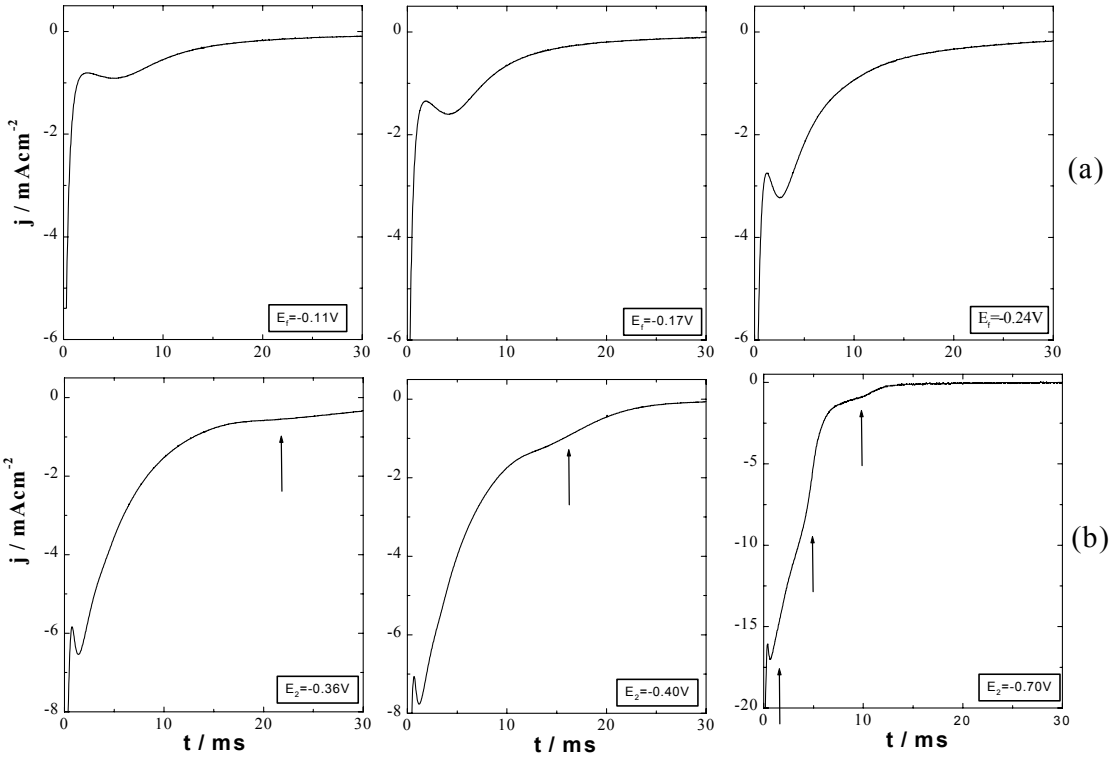


**Figure 4.10:** Current-time curves obtained after applying a single potential step from $E_i$ = 0.21 V (region IV) to various final potentials in: (a) region III; (b) the physisorbed film (region II). The waiting time at $E_i$ was 20 s. Remaining conditions identical as given in Figure 4.8: 14 mM thymine solution in 0.1 M $NaClO_4$ (pH = 6), T = 20 $^0$C.

In the model described to uracil dissolution, the proposed mechanism only takes in account reorientation of the adsorbed molecules with electron transfer and water desorption/adsorption. On the other hand, the current transients for $E_f$ inside the region II showed at least three processes which clearly indicates a more complicated dissolution mechanism as expected. Additionally, investigations at diluted thymine concentrations showed new features in the CV's (Figure 4.11).

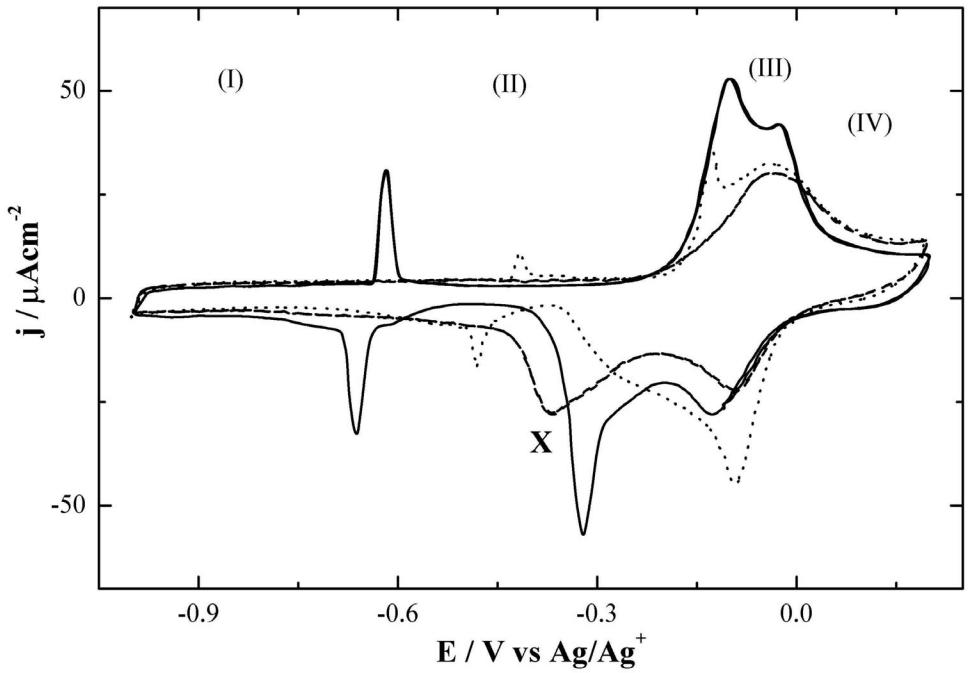


**Figure 4.11:** Cyclic voltammograms for 14 mM thymine (solid line), 2 mM thymine (dotted line) and 1 mM thymine (dashed line) in 0.1 M $NaClO_4$, pH = 6. Sweep rate: v = 200 mV/s. T = 20 °C.

As already known, at 14 mM thymine concentration the four well-defined regions for film formation/dissolution are well resolved. Decreasing the concentration to 2 mM the anodic scan still showed the formation of the four states, while during the cathodic scan the peak $T'_3$ disappeared. A further decrease of the concentration to 1 mM thymine leads to a totally different adsorption behavior compared to the one for 14 mM concentration. The peak pairs $T_1/T'_1$ vanished indicating that no physisorbed condensed film (region II) is formed on the electrode surface. However, a new cathodic peak is formed (peak X) around –0.36 V. The origin of this new peak is still not clear, but shows that a new process is obtained when the physisorbed condensed film is not formed. One can recognize three dissolution processes in the CV and in the transients curves (Figure 4.10 (b)).

## 4.2 URACIL

### 4.2.1 TAUTOMERISM AND pK VALUE

Uracil is a pyrimidine as thymine and its characteristics regarding the tautomeric forms and pKa are very close to thymine as can be seen (Figure 4.12). The only difference between uracil and thymine is the lack of the methyl group at C(5) in uracil.

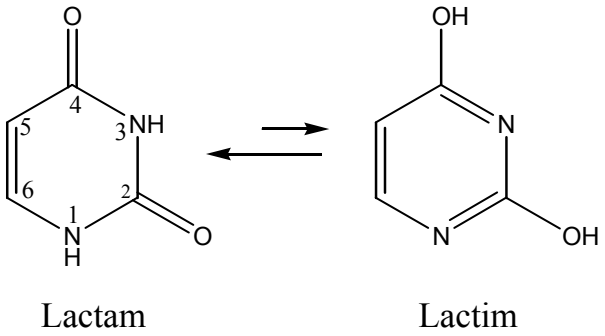


**Figure 4.12:** Tautomeric form for uracil.

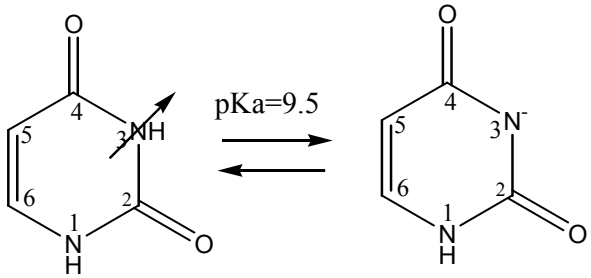


**Figure 4.13:** Ionization constant for uracil. The arrow indicates the dipole moment.

### 4.2.2 ADSORPTION OF URACIL ON AU(111)

Uracil adsorption on Au(111) showed adsorption states very similar to thymine (Figure 4.14) i.e., a non-condensed phase at a very negative potential (I) is followed by a two-dimensional physisorbed condensed film (II). Phase (III) reflects the transition from the physisorbed into the chemisorbed phase. In the capacity curve (Figure 4.14 (b)) is seen that the transition between phase I and II is characterized by a capacitance peak, which is smaller and broader as the comparable peak for thymine (Figure 4.3). This result corresponds to the needle peaks in the voltammogram of Figure 4.14 (a), which are not well resolved in case of

uracil condensation comparing with thymine condensation. Two reasons can be responsible for that difference. Either the density of the adsorbed layers between the random and the condensed adsorbed state is smaller or the kinetics formation of the condensed state is slow in case of uracil in comparison to thymine. Once the peak positions are nearly independent of the scan value; we tend to accept the first explanation for this behavior, i.e., that the of the peaks $T_1/T'_1$ indicates the presence of nucleation and growth process [74]. In contrast, the capacity peaks corresponding to the transition between state II and IV indicate a process faster than the corresponding one in the thymine system. The capacitance state of phase IV (11 $\mu$ $Fcm^{-2}$) is neither concentration nor temperature dependent.

During the transition for state II to IV the molecules undergo a reorientation connected with a partial charge transfer. *In-situ* STM measurements on Au(111) and Au(100) for the physisorbed films confirm that uracil forms a two-dimensional network of planar oriented molecules stabilized by hydrogen bonding independently of the substrate geometry. At very positive potentials a chemisorbed phase is formed (IV). The uracil molecules form a surface coordination complex resulting in a highly organized two-dimensional structure [78], whereby the molecules are oriented in a up right position regarding to the electrode surface. The configuration and hydrogen bonding observed within the molecules were very similar to those found in the 3D crystal [79].

Sowerby *et al.*[11] investigated the structure of 2D thymine and uracil adsorbates on $MoS_2$ and highly oriented pyrolytic graphite (HOPG) electrodes. It was suggested that on both surfaces the two-dimensional hydrogen bonding networks are almost identical with intermolecular configurations, as observed in their respective three-dimensional crystals.

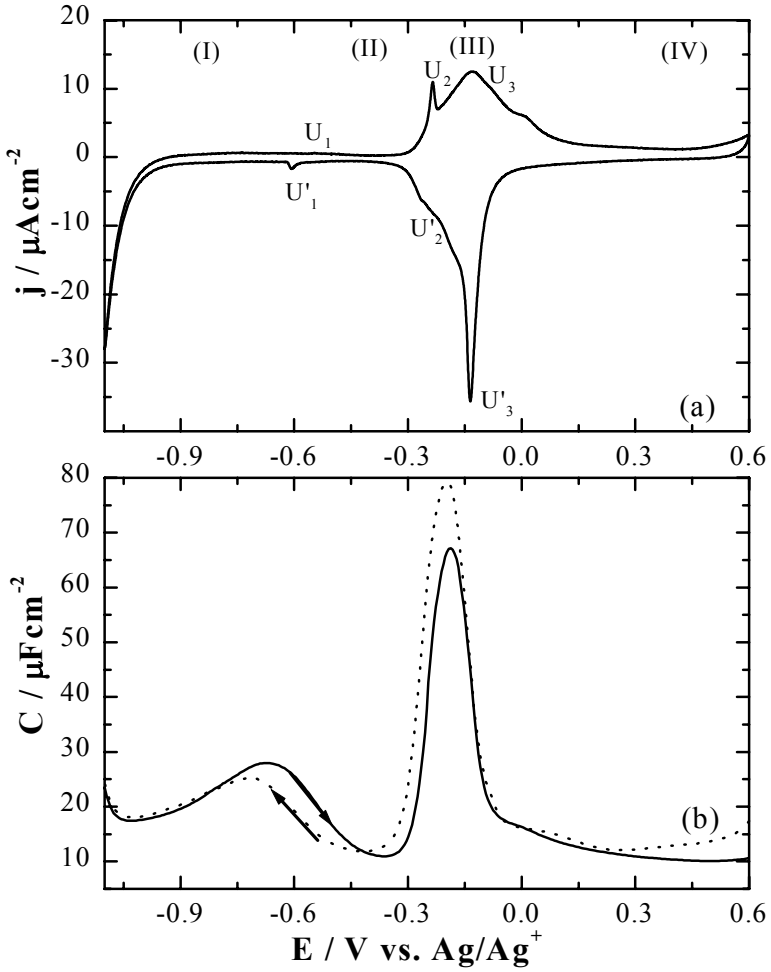


**Figure 4.14:** Cyclic voltammogram of 6 mM uracil (a) and capacity curves(b). $U_1/U'_1$ and $U_2/U'_2$: formation and dissolution of ordered physisorbed uracil monolayer; $U_3/U'_3$ formation and dissolution of the ordered chemisorbed uracil monolayer. Supporting electrolyte: 0.1 M $NaClO_4$ (pH = 2). Sweep rate: v = 50 mV/s (a) and v = 5 mV/s (b). Perturbation frequency and amplitude when measuring the capacity curve: 20 Hz, and 3 mV, respectively. T = 20 °C.

Lowering the uracil concentrations (Figure 4.15) the needle peaks at negative $U_1/U'_1$ and positive potentials $U_2/U'_2$ disappeared. As the surface coverage of adsorbate molecules depends on the electrode potential as well as on the concentration of the molecules in the electrolyte, the absence of these peak pairs indicates that the critical concentration of thymine molecules necessary to form a condensed layer by a phase-transition process at this temperature is not reached.

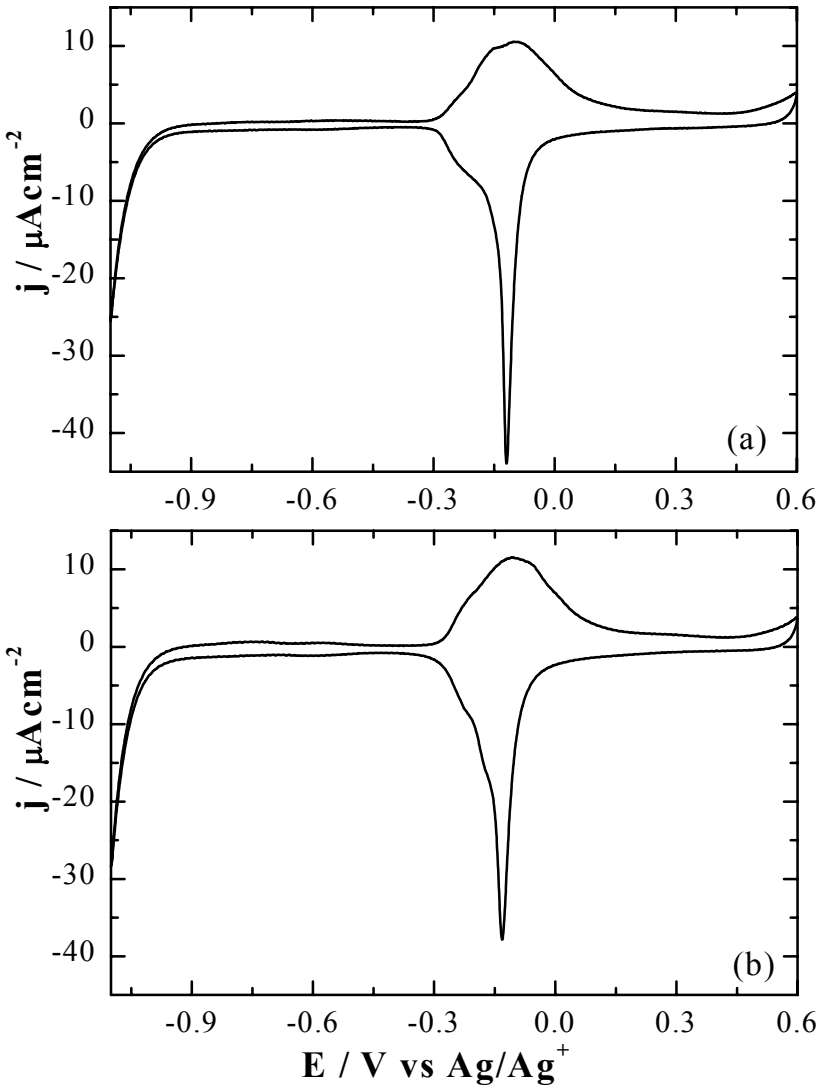


**Figure 4.15:** Cyclic voltammograms of uracil 1 mM (a) and uracil 3 mM (b). Supporting electrolyte: 0.1 M $NaClO_4$ (pH = 2). Sweep rate: v = 50 mV/s. T = 20 $^oC$.

## 4.3 ADENINE

Adenine or 6-aminopurine is one the most common nucleic acid base found in the DNA and RNA, which is directly involved in protein synthesis and in the transfer of the genetic information. Adenosine triphosphate (ATP) is one of the so-called energy rich group compounds because it exhibits a large decrease of free energy when undergoes certain hydrolytic reactions [106]. Adenine also occurs as a component of a number of coenzymes, for example coenzyme I: is nicotinamide adenine dinucleotide ($NAD^+$) or diphosphopyridine

nucleotide ($DPN^+$), coenzyme II is nicotinamide adenine dinucleotide phosphate ($NADP^+$) or triphosphopyridine nucleotide ($TPN^+$). Coenzymes of these types are often involved in oxidation-reduction process in biological reactions together with the appropriated enzyme and therefore have a particular interest to be investigated under electrochemical conditions.

### 4.3.1 TAUTOMERISM AND pK VALUES

Adenine is derivated from simple purine by replacing the hydrogen at 6 position by an amino group ($NH_2$). The heterocyclic molecules in solution generally yield a mixed population of species in equilibrium when the hydrogen atoms attached to nitrogen are able to migrate to other free nitrogen or oxygen within the same molecule (prototropic change). This kind of tautomerism depends on the dieletric constant of the solvent and on the pK value of the heteroatoms. The tautomeric forms from adenine are the *amine* and *imino* form (Figure 4.16), respectively.

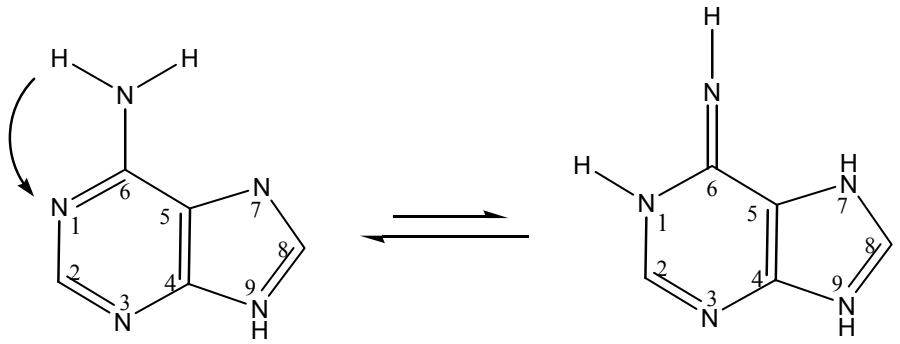


**Figure 4.16:** Tautomeric equilibrium of adenine.

Although adenine can undergo a change from an amine to an imino form, the amine form is strongly favored being more difficult to detect even traces of the imino form in the naturally occurring DNA. However, if the less stable form is present in DNA it can seriously alter the DNA sequence by forming base pairs other than the standard ones. Normally, adenine and thymine form the AT standard pairs, however the imino form from adenine can form a stable hydrogen bonded pair with cytosine, AC instead of AT, causing a mutation process.

At lower pH adenine undergoes protonation on the N(1) position rather than on the amino group. The charged form is stabilized by the resonance hybrids (Figure 4.17).

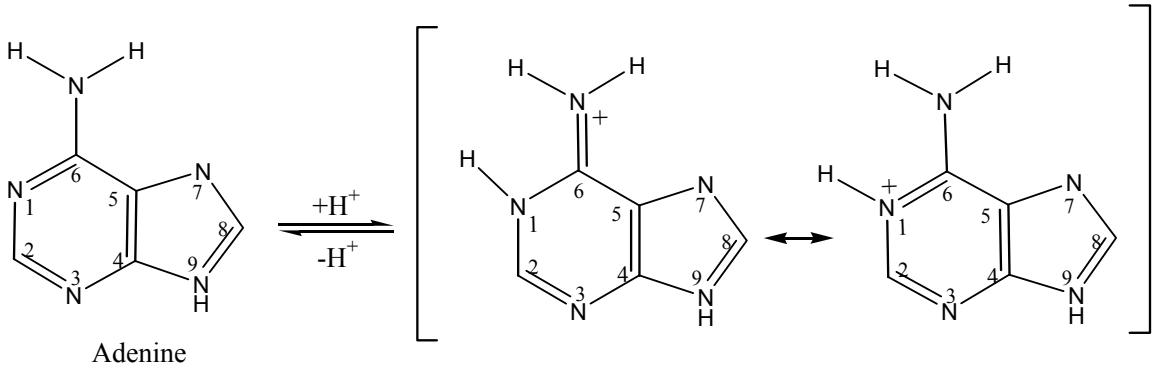


Adenine

**Figure 4.17:** Protonated forms of adenine.

Crystallographic studies have shown that at pH < 2 adenine is double protonated at N(1) and N(7) nitrogen and the bonding geometry is changed according to the resonance structures.

In living cells, the interaction of nucleic acids with the electric field of charged membranes has a fundamental biological importance [79,80]. The electrode surface can be regarded as a biological membrane and represents therefore a model system, which is suitable for investigations of the interaction of biological molecules with charged interfaces.

Vetterl *et al.* [20,21] were the first who investigated the effect between the electric field and adenine adsorption on Hg electrodes. At negative potentials in acidic solution, they observed a negative capacity pit, which is interpreted as the association of protonated adenine molecules through the positive charge on N(1) and the electrode surface negatively charged. Adenine presents two pKa values as can be seen in Figure 4.18.

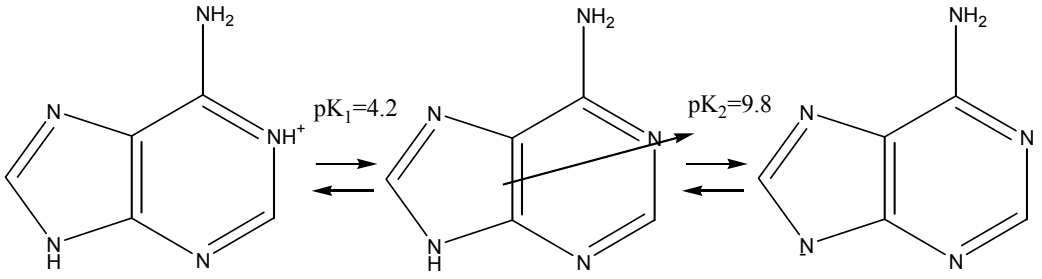


**Figure 4.18:** Adenine pKa values. Arrow denotes the dipole orientation.

That means that the best condition to obtain an association of adenine and the negatively charged electrode surface is the pH near the $pK_1$ (Figure 4.18). In later papers this up right orientation or flat orientation on mercury could not be confirmed. It is now well accepted that even on mercury electrodes the adenine molecules are flat orientated in the condensed adsorption state [31]. But to compare thymine and adenine adsorption behavior in the present work all measurements in adenine solution were performed at pH = 2 and pH = 6, where most of the adenine is protonated or neutral, respectively.

### 4.3.2 ADSORPTION OF ADENINE ON AU(111) AND ON AU POLYCRISTALLINE

The interfacial behavior of adenine on Au(111) was studied mainly by STM [14] and SERS [81] measurements. Detailed electrochemical data of this system were not available from the literature. Therefore we had to study some relevant aspects regarding to adsorption behavior of this system before entering the coadsorption problem between the complementary base pairs adenine-thymine.

Many authors report on the adsorption behavior of adenine at mercury electrodes [82-86] but, to our knowledge, only few electrochemical studies were performed on the adsorption behavior of adenine at Au(111) electrodes [12,14,81,87].

When comparing the adsorption behavior of thymine and adenine on mercury electrodes, two features attract more attention. At first, adenine adsorbs considerably stronger than thymine. Secondly, the position of the condensation region for adenine is located at more positive potentials in comparison to thymine. Likewise, adenine undergoes a reorientation during the phase transition whereby the reorientation causes a PZC shift in negative direction [31].

Additionally, at lower pH values a second adsorption region was obtained at very negative potentials. Since at pH values smaller than 4.2 more than 50% of adenine is available in its protonated form, Janik et al. explained this second adsorption region by the electrostatic interaction between the protonated adenine and the negatively charged mercury electrode [88]. Giese and McNoughton [89] investigated the adenine adsorption on colloids, roughened electrode and island films of silver by SERS and DFT calculations suggesting that adenine interacts with different orientation depending on the surface. In the colloidal system adenine adsorbs perpendicular to the surface via N(7) and the amino group. At electrode,

adenine is more tilted orientated, but still interact via N(7) and via the amino group. On silver island films, adenine interact also in a tilted orientation, but more via the amino group.

In the same way, on Au(111) electrodes adsorbs in different orientations depending on the applied potential. The interpretation is mainly based an experiment done by Xiao *et al.* [81] who investigated the potential dependent adsorption of nicotinamide adenine dinucleotide ($NAD^+$) on roughened Au electrode by SERS measurements. Based on the difference in SERS spectra at negative and positive potential region, they concluded that under negative potential the adenine moiety of NAD is adsorbed in a flat orientation forming a charge-transfer complex between the LUMO of adenine and the d-orbital of Au(111). In contrast, at positive charged electrode the adenine moiety is adsorbed in a vertical orientation with contact to the Au(111) by the $NH_2$ group.

The adsorption behavior of adenine on Au(111) differs from that of thymine on Au(111) as well as that of adenine on mercury electrodes (Figure 4.19).

Adenine adsorption on Au(111) causes three peak pairs, $A_1/A'_1$, $A_2/A'_2$ and $A_3/A'_3$ (Figure 4.19). In contrast to thymine (Figure 4.3), where the peak pairs $T_1/T'_1$ and $T_2/T'_2$ define the stability region for the physisorbed condensed monolayer, no corresponding needle peaks are observed in the adenine system. But it should be mentioned that in a very diluted acidic adenine solution a reproducible positive needle peak is observed in the negative scan direction at a very negative potential region, where the reduction of water starts (Figure 4.19c). The same result was obtained by Rueda and coworkers for the adenine adsorption on Au(111) in a neutral electrolyte [87]. The origin of this small reproducible peak is not clear. A more detailed characterization is difficult, because at higher adenine concentration the peak disappeared, or, alternatively, is shifted to more negative potentials, so that the water reduction makes its detection impossible. On the other hand, at higher pH values the water reduction shifts to more negative potentials, but simultaneously the peak pairs $A_1/A'_1$, $A_2/A'_2$ also shift to negative direction (Figure 4.21). Therefore, also at higher pH values this needle peak cannot be observed.

The position of the broad peak pairs ($A_1/A'_1$ and $A_2/A'_2$) depends only slightly on the bulk adenine concentration in a range between 2 mM and 0.08 mM (Figure 4.20). This behavior indicates that the surface obviously is completely covered with adenine at potentials positive and negative of these peak pairs. The position of the peak pair $A_3/A'_3$ remains unchanged by decreasing the adenine concentration but their intensity becomes enhanced.

The positions of all of the peak pairs depend strongly on the pH value. At pH = 6 (Figure 4.21) the peak pairs are shifted to lower potentials in comparison to pH = 2 (Figure 4.19). Additionally, the current density for the peaks $A_1/A'_1$ and $A_2/A'_2$ increases with increasing pH value. It should be mentioned that adenine is protonated at pH = 2, whereas at pH = 6 the neutral form of adenine dominates.

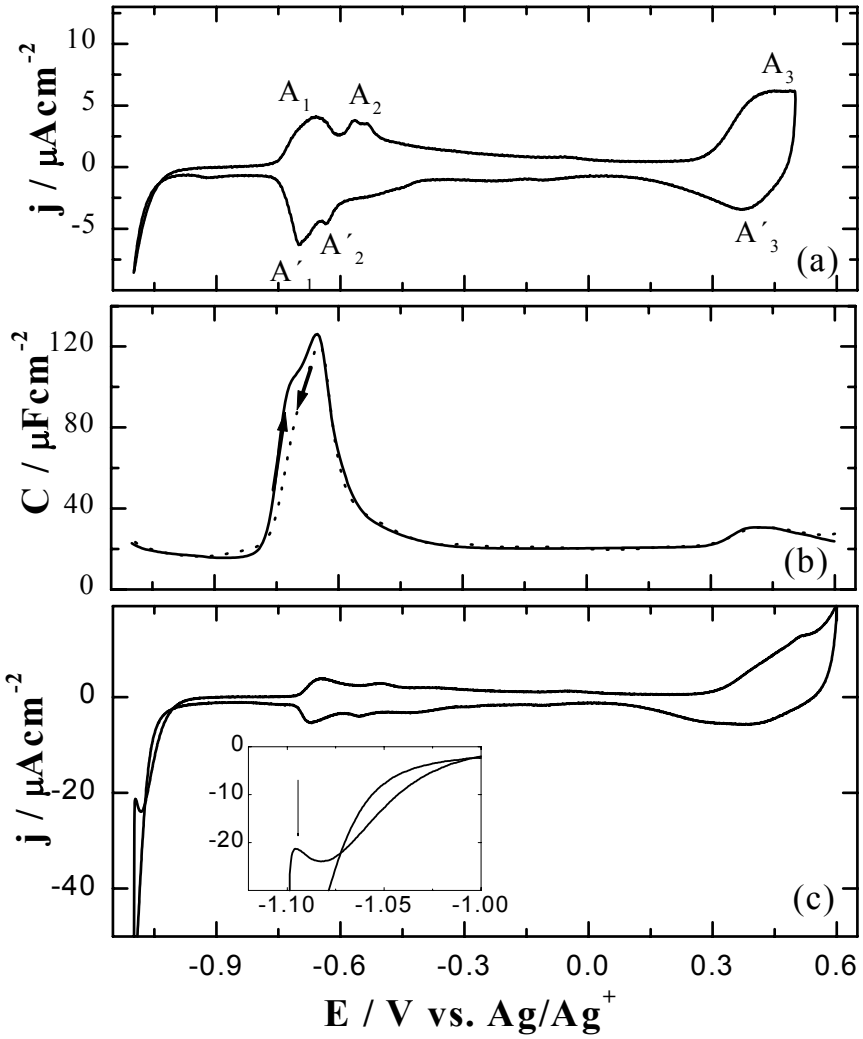


**Figure 4.19:** Cyclic voltammogram of 2 mM adenine (a), capacity curve (b), and CV of adenine 0.08 mM (c). $A'_1/A'_2$ and $A_1/A_2$: formation and dissolution of the charge-transfer complex between the π*-orbital of adenine and d-orbital of the gold surface; $A_3/A'_3$ oxidation of gold in the Au-adenine complex. Supporting electrolyte: 0.1 M $NaClO_4$ (pH = 2). Sweep rate: v = 50 mV/s (a) and (c) and v = 5 mV/s (b). Perturbation frequency and amplitude when measuring the capacity curve: 80 Hz, and 3 mV, respectively. T = 20 °C.

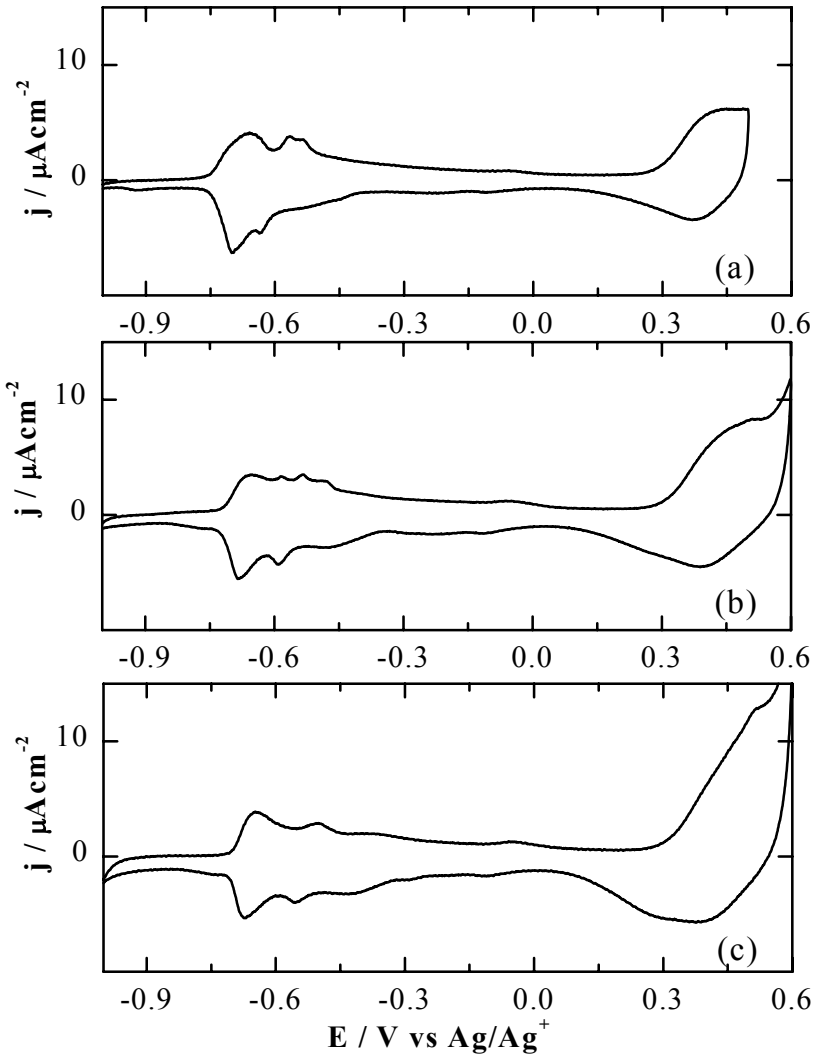


**Figure 4.20:** Cyclic voltammograms of adenine 2 mM (a), adenine 0.4 mM (b), and adenine 0.08 mM (c) in 0.1 M $NaClO_4$, pH = 2, T = 20 °C, scan rate 50 mV/s.

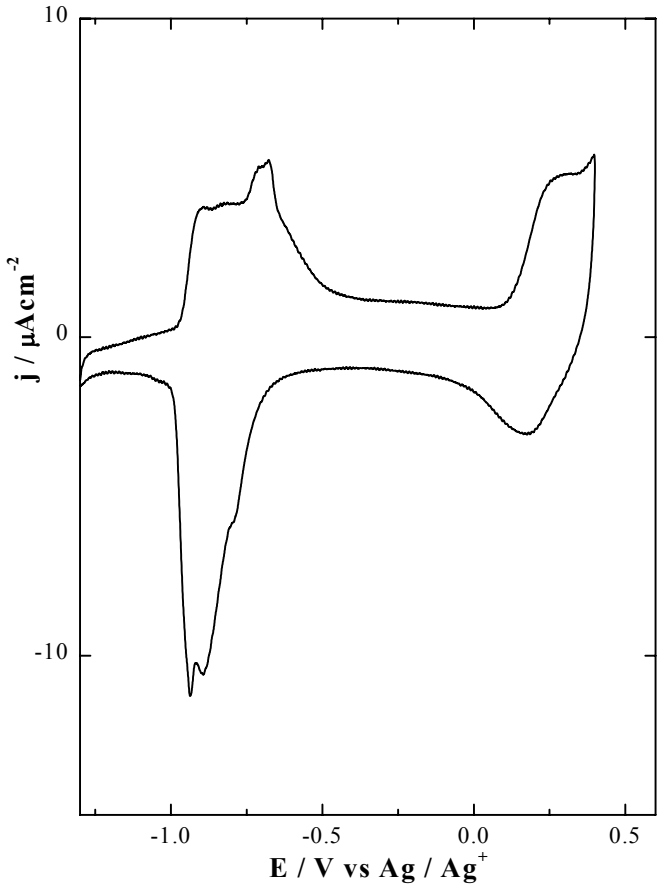


**Figure 4.21:** Cyclic voltammogram of adenine 1 mM in 0.1 M $NaClO_4$, pH = 6, T = 20 °C, scan rate 50 mV/s.

The adsorption of adenine on Au(111) (0.05 M $NaClO_4$, pH = 7) and on graphite (HOPG) (0.1 M NaCl, NaJ, pH = 7) has been investigated by STM under electrochemical conditions [12,14]. In addition, there exists a SERS study [81] on the adsorption of adenine at polycrystalline Au. The direct comparison of the data obtained by these experiments with the results given here is difficult. The STM figures reveal that (at least at graphite) the molecular plane of adenine is oriented parallel to the surface of the electrode at negative potentials, whereas at positive potentials the plane of the molecule is oriented perpendicular to the surface. Unfortunately, the electrochemical data available [14], are hardly comparable with our results, especially because the peak pairs $A_1/A'_1$ and $A_2/A'_2$ were not observed, whereas, Rueda [87] found these peak pairs in electrochemical studies (pH = 7). For a more detailed discussion of the adenine adsorption on gold, the SERS study of Xiao [81] reveals further important results. He found, in agreement with the STM studies, that at positive potentials (> -0.1V) a direct contact of the $NH_2$-group and N(7) with the surface exists. At negative

potentials (-0.9 V) the π-system of adenine is in contact with the surface. In this state a charge transfer complex is formed in which a partial electron transfer from the gold d-orbital to the □*-orbital of adenine is assumed.

In accordance with this model we identified the broad peaks $A'_1/A'_2$ in Figure 4.19 as the formation and the peaks $A_1/A_2$ as the dissolution of the charge transfer complex between the adsorbed protonated adenine and the gold surface. At pH = 6 adenine exists in its neutral form. Due to the deprotonation of adenine in the N(1) position, the energy of the lowest □*-orbital increases. This lowers the stability of the Au-adenine charge transfer complex, which is expressed by a shift of the peak pairs to more negative potentials by about -0.22 V (Figure 4.20).

Up to now, only a tentative interpretation of the signals $A_3/A'_3$ at about 1 V (SCE) can be given (Figure 4.19). These peaks appear about 100 mV more negative than the gold oxidation in the pure electrolyte. We assume that in this potential range also an adenine-gold complex is formed. The adenine orientation regarding the electrode surface at this potential points to an interaction of lone pair electrons of adenine with the gold surface favorable for a partial electron transfer from adenine to gold. This is comparable to the formation of the chemisorbed layer of thymine at gold [71], but the adenine-gold complex causes a strong shift of the onset of gold oxidation to more negative potentials. This explains that the current positive of the peak $A_3/A'_3$ increases considerably. From the signal shifts to more negative potentials with increasing pH values (Figure 4.20) it can be concluded that a deprotonation step is involved, as observed with thymine.

Summarizing, it can be stated that two adsorption states of adenine on Au(111) exist. At potentials negative of the peak pairs $A_1/A'_1$ and $A_2/A'_2$ a chemisorbed charge transfer complex is formed which is oriented parallel with respect to the surface, whereas at potentials positive of the peak pairs $A_1/A'_1$ and $A_2/A'_2$ adenine is adsorbed perpendicular to the plane of the electrode.

Comparing the adsorption behavior of adenine on Au polycrystalline and Au(111) surface, the cyclic voltammogram measured at polycrystalline Au do not show any well defined peak for the negative and positive potentials (Figure 4.22). Only a broad capacity current occurs in the whole double layer region, whereby a small peak at about –0.5 V can be recognized. In contrast, a careful analysis of the capacity curves gives a better idea about the adsorption process.

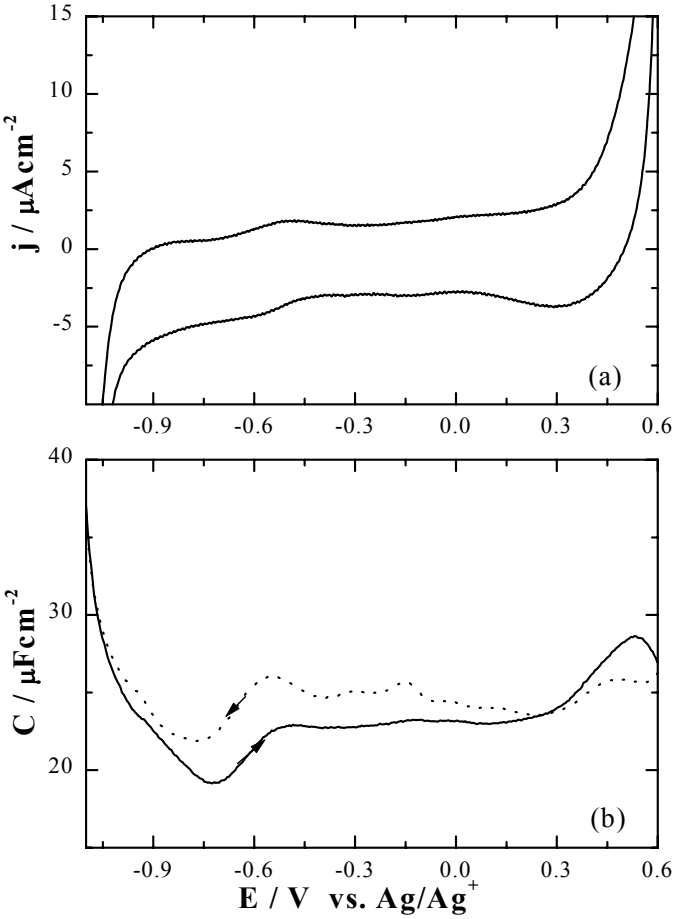


**Figure 4.22:** Cyclic voltammogram of polycristalline gold in 3 mM adenine on (a) and capacity curves (b). Supporting electrolyte: 0.1 M $NaClO_4$. Sweep rate: v = 50 mV/s (a) and v = 5 mV/s (b). Perturbation frequency and amplitude when measuring the capacity curve: 80 Hz, and 3 mV, respectively. T = 20 $^oC$.

Analyzing the capacitive curve in the forward scan (solid line) in Figure 4.22 (b), a minimum appeared at negative potentials, at the same potentials where for the Au(111) surface the formation of adenine π*-complex was assumed. This result supports our conclusions that adenine is stronger adsorbed in the negative than in the positive potential region.

## 4.4 COADSORPTION OF THYMINE AND ADENINE ON AU(111) AND ON AU POLYCRISTALLINE

All the information that our descendents needs is stored inside the cell in form of the genetic code. As we already know, each unit of DNA is composed by nucleotides, formed by a sugar, a phosphate group and by the nitrogened bases (adenine (A), thymine (T), cytosine (C) and guanine (G)). The alignment of the nucleotides forms two strands and the combination of the nitrogened bases are responsible for all the genetic information necessary to give rise to a unique individual with their own characteristics. The nitrogen bases in the one strand form hydrogen bondings with the bases of the other strand forming the so-called complementary base pairs. For the DNA, these allowed pairs are A-T and C-G.

Keeping in mind these interactions in the DNA, the question arises: is it possible to obtain the same interaction between complementary base pairs A-T at charged surfaces, conveniently studied by appropriated electrochemical methods?

The coadsorption behavior of adenine-thymine was first investigated on mercury electrodes [31], where the authors did not find a mutual interaction between the bases. That means that the interaction between the bases alone is stronger than in the mixed solution.

As it is known from the adsorption behavior on mercury [31] electrode adenine is adsorbed much stronger than thymine. Therefore, we started our experiments at the Au(111) electrode at bulk concentrations of adenine (2 mM) and thymine (20 mM) in an acidic electrolyte solution (pH = 2). For this concentration ratio and pH value the chemisorption of pure adenine takes place in a potential region where pure thymine is physisorbed (Figure 4.23). Starting with these concentrations, the coadsorption behavior of thymine / adenine is shown in Figure 4.24. The needle peaks $T_1/T'_1$ indicating the first-order phase transition of thymine in the physisorbed phase could not be obtained. Instead of the well-resolved peaks $T_2/T'_2$ and $T_3/T'_3$ showing the transition form state II to IV of thymine at –0.214V (Figure 4.23), a broad signal appears ($T_{2/3}/T'_{2/3}$, Figure 4.24). These results give an indication, as expected, that the absolute concentration of thymine at the surface is lower due the coadsorption than in pure thymine solution. In contrast to the broad chemisorption peaks of adenine ($A_1/A'_1$ and $A_2/A'_2$) observed in a pure adenine solution, their shapes are changed significantly in the mixture ($AT_1/AT'_1$ and $AT_2/AT'_2$). In Figure 4.24a it can be clearly distinguished between two well-separated peaks in both directions, whereas in Figure 4.23b

these peaks are hardly resolved, but their position remains nearly unchanged in comparison to $A_1/A'_1$ and $A_2/A'_2$. The shape of these peaks is influenced by the concentration ratio of adenine/thymine (Figures 4.24 and Figure 4.26), by the temperature (Figure 4.30) and the pH value of the solution (Figure 4.25).

Starting from an thymine/adenine ratio of 20 mM / 3 mM a decrease of the adenine concentration to 2 mM do not change neither the position nor the shape of the peak pairs $AT_1/AT'_1$ and $AT_2/AT'_2$ (Figure 4.24 (a) and (b)). On the other hand, a decrease of the thymine concentration to 10 mM at an adenine concentration of 2 mM leads to a CV (Figure 4.24(c)), which resembles the voltammogram for a pure adenine solution. A further decrease of the adenine concentration to 1 mM, in that case that the ratio thymine/adenine is 10 mM / 1 mM (Figure 4.24(d)), the obtained CV is very similar to that presented in Figure 4.24(a). It seems that a critical ratio of the surface concentration of thymine and adenine must be reached (1 mM / 10 mM) in order to obtain a measurable effect on the chemisorption kinetics representing by the peak pairs $AT_1/AT'_1$ and $AT_2/AT'_2$. At pH = 6 this measurable effect is obtained at lower thymine / adenine ratios.

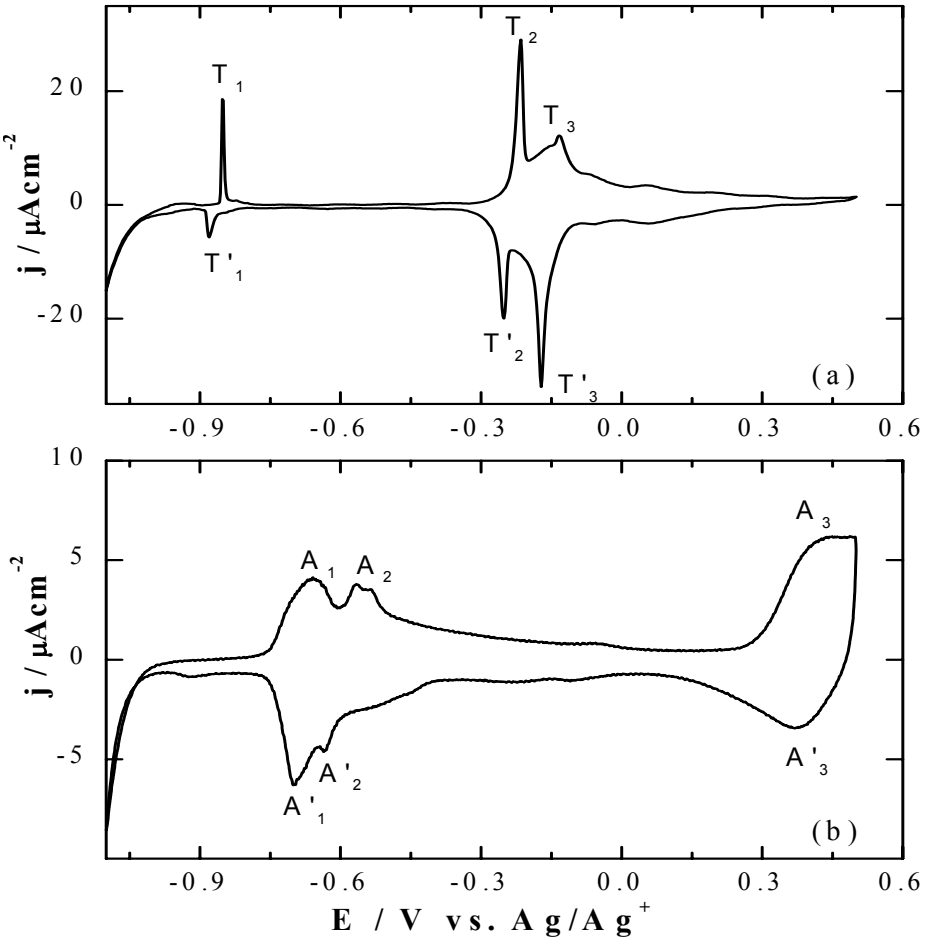


**Figure 4.23:** Cyclic voltammograms of 20 mM thymine (a) and 2 mM adenine (b) in 0.1 M $NaClO_4$, pH = 2, T = 20 °C, scan rate 50 mV/s. $T_1/T'_1$: formation and dissolution of the ordered physisorbed thymine monolayer; $T_2/T'_2$: dissolution and formation of the ordered physisorbed thymine monolayer; $T_3/T'_3$: formation and dissolution of the ordered chemisorbed thymine monolayer; $A'_1/A'_2$ and $A_1/A_2$: formation and dissolution of the charge-transfer complex between the $\pi^*$-orbital of adenine and d-orbitals of the gold surface; $A_3/A'_3$ oxidation of gold in the Au-adenine complex.

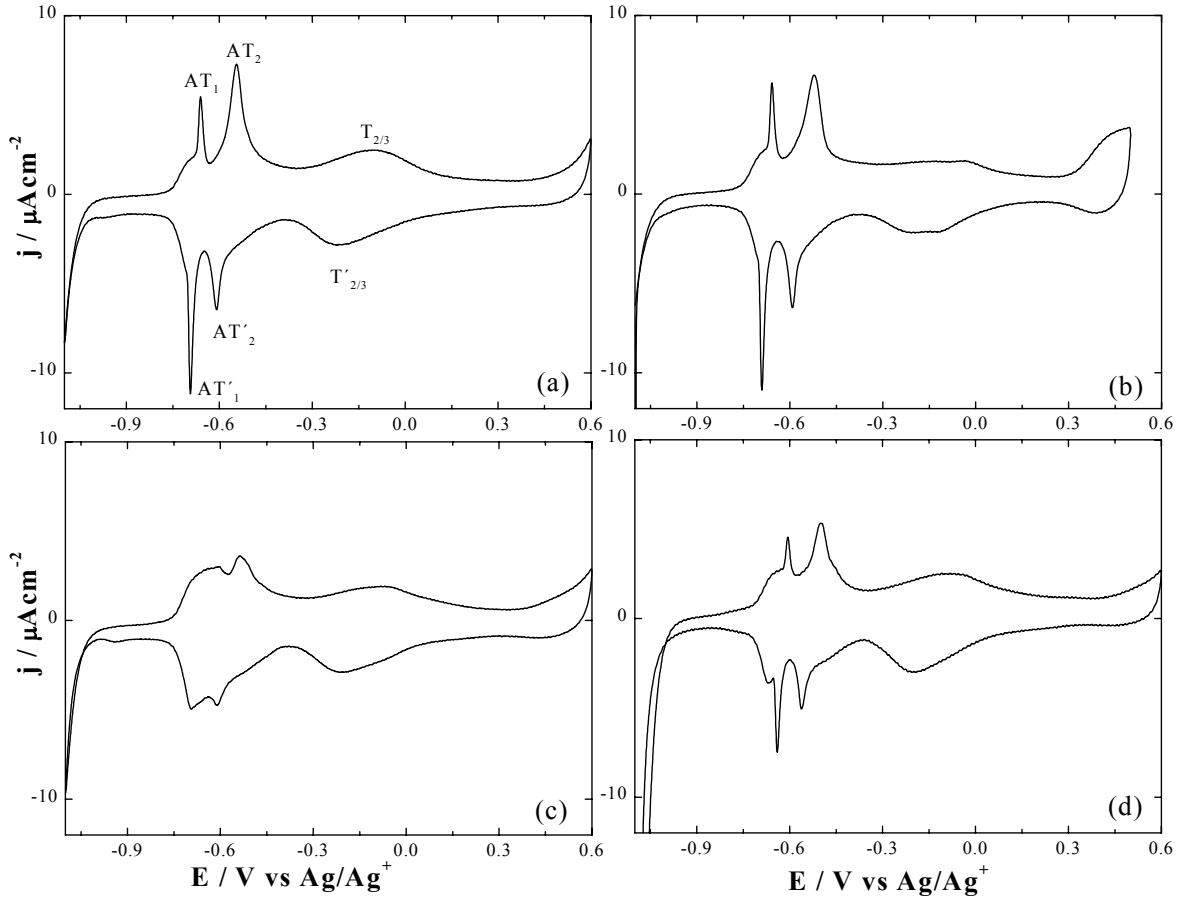


**Figure 4.24:** Cyclic voltammogram of thymine 20 mM + adenine 3 mM (a); thymine 20 mM + adenine 2 mM (b); thymine 10 mM + adenine 2 mM (c) and thymine 10 mM + adenine 1 mM (d) in 0.1 M $NaClO_4$, pH = 2, T = 20 °C, scan rate 50 mV/s. $AT_1/AT_2$ and $AT'_1/AT'_2$: dissolution and formation of the charge-transfer complex between the π*-orbital of the A-T complex and the d orbital of the gold Au(111) surface.

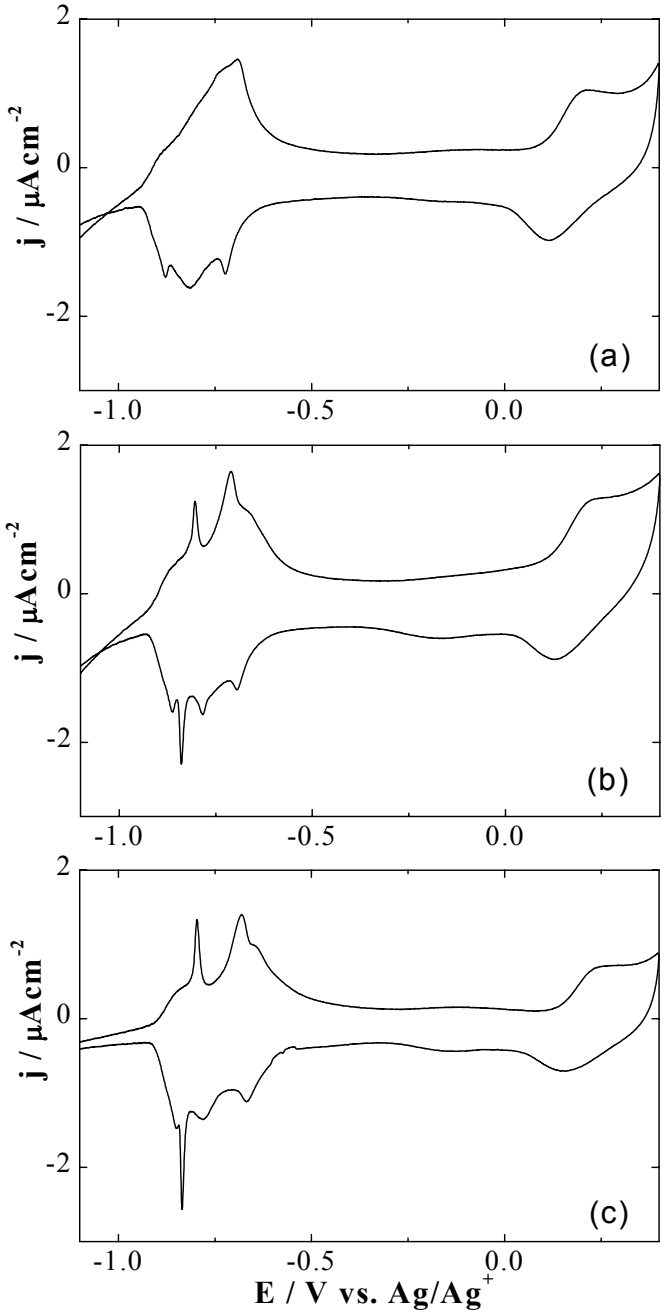


**Figure 4.25:** Cyclic voltammogram of thymine 20 mM + adenine 2 mM (a); thymine 20 mM + adenine 1 mM (b); and thymine 20 mM + adenine 0.5 mM (c) in 0.1 M $NaClO_4$, pH = 6, T = 20 °C, scan rate 50 mV/s.

A decrease of the adenine concentration at a given thymine concentration of 20 mM (pH = 2) reveals new features in the CVs (Figure 4.26). The peak pairs $AT_1/AT'_1$ and $AT_2/AT'_2$ are broadened and shifted to more positive potentials by several tens of mV (table 1), with decreasing adenine concentration.

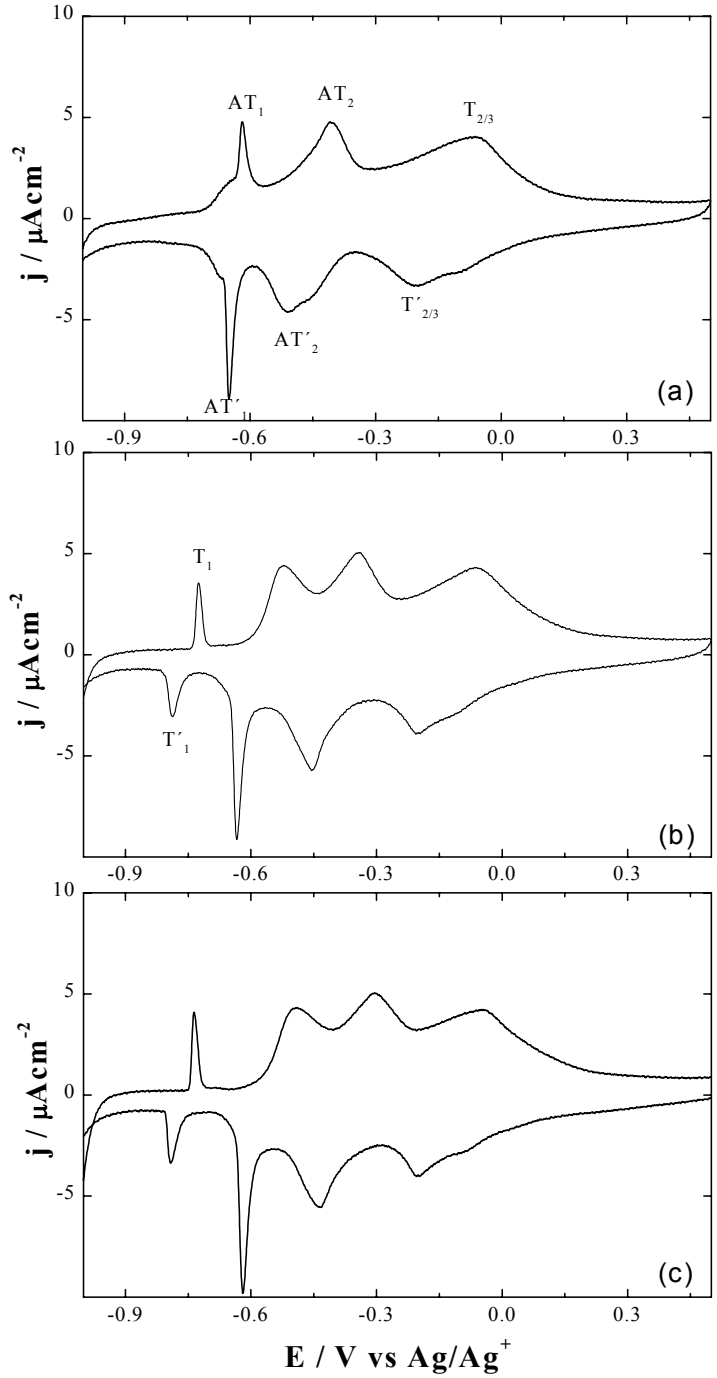


**Figure 4.26:** Cyclic voltammogram of thymine 20 mM + adenine 0.4 mM (a); thymine 20 mM + adenine 0.08 mM (b); and thymine 20 mM + adenine 0.06 mM (c) in 0.1 M $NaClO_4$, pH = 2, T = 20 °C, scan rate 50 mV/s.

**Table I:** Peak potentials to formation and dissolution of the A-T charge-transfer complex. The thymine concentration is 20 mM, v = 50 mV/s, pH = 2.

| [A]/mM | FORMATION | | DISSOLUTION | |
|---|---|---|---|---|
| | $AT'_1$/mV | $AT'_2$/mV | $AT_1$/mV | $AT_2$/mV |
| 3 | -697 | -605 | -659 | -545 |
| 2 | -687 | -590 | -650 | -519 |
| 0.4 | -650 | -507 | -615 | -402 |
| 0.08 | -638 | -453 | -521 | -342 |
| 0.06 | -617 | -431 | -494 | -301 |

To have a better idea how the peaks AT (for adenine-thymine complex formation/dissolution), as well as the peaks T (for formation/dissolution of thymine physisorbed film) shift the potentials depending on adenine concentration, the Figure 4.27 is shown. Increasing the adenine concentration, the peak pairs regarding to formation and dissolution of a charge-transfer-complex between the π*-adenine and the gold surface (AT / AT') shift to more negative potentials. On the other hand, the phase transition peaks indicating the formation / dissolution of the thymine physisorbed film (T / T') shifted to more positive potentials higher the adenine concentration is. That means that the formation of physisorbed thymine films at the electrode surface is disturbed by adding adenine.

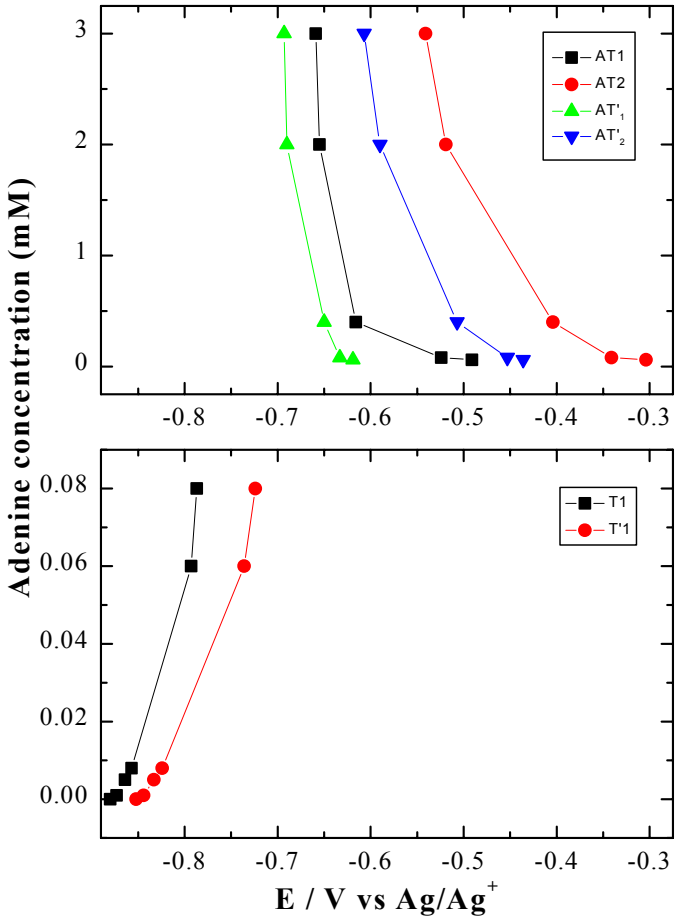


**Figure 4.27:** Peak potential variation with adenine concentration for thymine and adenine solution. Thymine concentration is fixed at 20 mM, pH = 2, T = 20 °C, V = 50 mV/s.

At a concentration ratio of thymine/adenine of 20 mM / 0.08 mM and lower the peak pair $T_1/T'_1$ is observed, which clearly indicates the formation and dissolution of the pure condensed physisorbed thymine film. Finally, at very low adenine concentration (0.001 mM, Figure 4.28) a CV results which seems to be identical with that of a pure thymine solution. But a detailed inspection of the peak pair $T_1/T'_1$ (Figure 4.29) reveals that even at this very low concentration the formation and dissolution of the thymine film is influenced by adenine as can be seen by the small shifts of these peaks to positive potentials in comparison to their position in the pure thymine solution.

The broad signals $T_{2/3}/T'_{2/3}$ are correlated with the formation and dissolution of the chemisorbed and physisorbed thymine phase, respectively. With decreasing adenine concentration this peak pair splits into separated signals.

Figure 4.30 shows the adsorption behavior of the adenine/thymine system with different concentration ratios at 10 °C. It should be compared with Figure 4.26, which shows the behavior of this system at 20 °C. At 10 °C the peak pair $T_1/T'_1$ is observed at an A/T ratio of 0.4 mM / 20 mM in contrast to the measurement at 20 °C, where this peak pair is recognized at the A/T ratio 0.08 mM / 20 mM. This shows that the adenine adsorption or the kinetics of the adenine adsorption depends stronger on the temperature than the thymine adsorption.

Finally, we observed that the variation of the equilibrating time at the negative starting potential at -0.38 V (Figure 4.31) between 30s and 30min does neither influence the peak positions nor the peak height in a significant manner. The variation of the scan rates between 10 and 100 mV/s do not influence the peak positions.

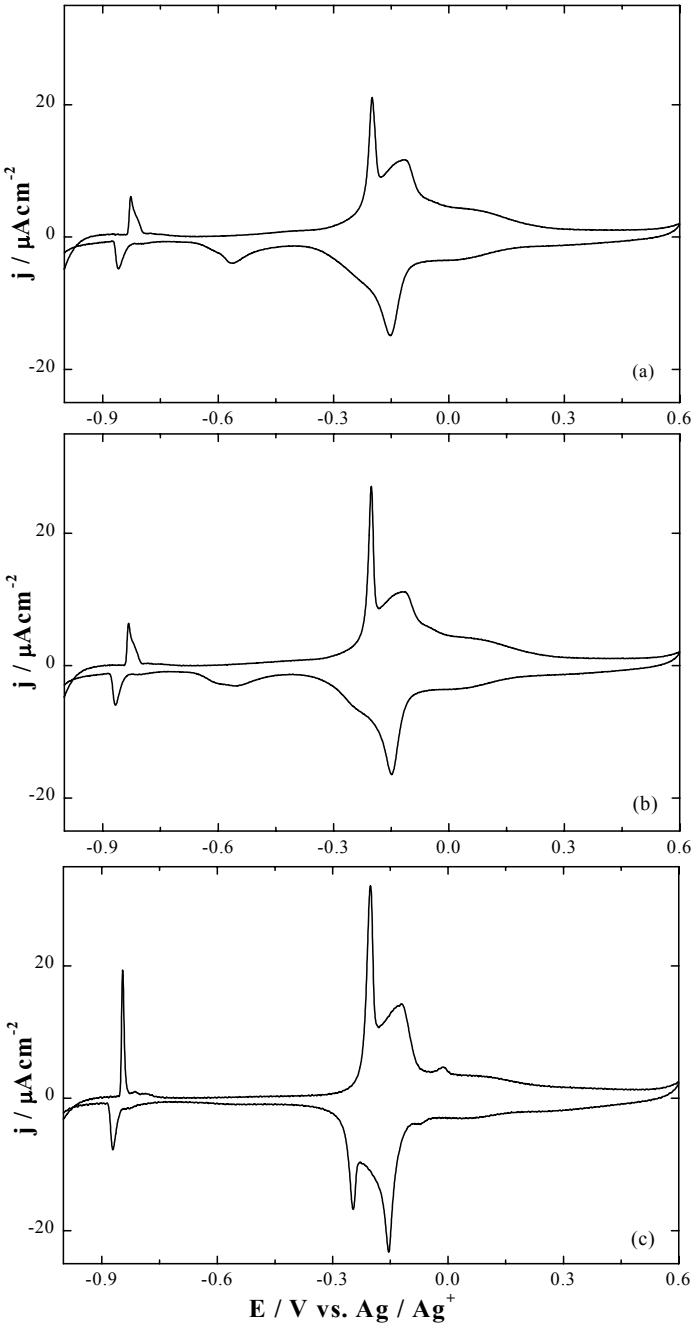


**Figure 4.28:** Cyclic voltammogram of thymine 20 mM + adenine 0.008 mM (a); thymine 20 mM + adenine 0.005 mM (b); and thymine 20 mM + adenine 0.001 mM (c) in 0.1 M $NaClO_4$, pH = 2, T = 20 °C, scan rate 50 mV/s.

Despite the strong adsorption of adenine and the high thymine bulk concentration it could not be observed that one of both molecules replaces the other one in a measurable time scale.

It should be mentioned that after cycling into the potential region where gold oxidation/reduction takes place it was not possible to electrochemically detect any peaks in the negative back scan.

At positive potentials not only oxidation/reduction but also the change between the reconstructed and the unreconstructed surface states on single crystal electrodes affects the electrode surface. Whether the reconstructed or unreconstructed surface is stable depends on the potential [90-92] as well as on the electrolyte composition and adsorbates [90,93-95]. Also, it is known that a potential induced reconstruction leads to less ordered surface states than a thermally induced reconstruction.

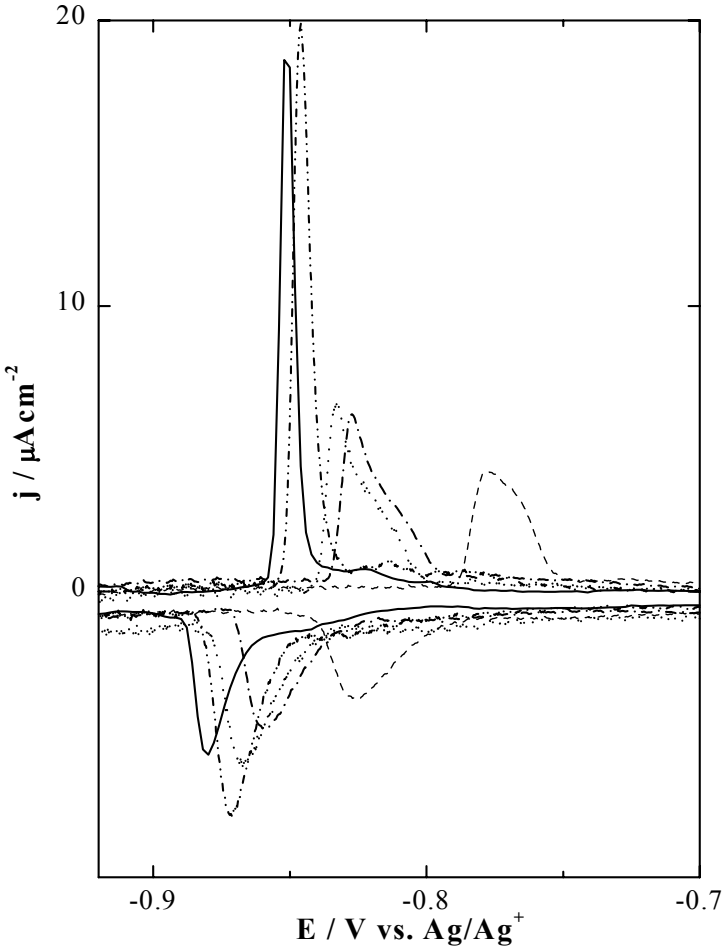


**Figure 4.29:** Needle peaks of thymine 20 mM (solid line); thymine 20 mM + 0.001 mM adenine (dash dot dot line); thymine 20 mM+ 0.005 mM adenine (dot line); thymine 20 mM + 0.008 mM adenine (dash dot line) in 0.1 M $NaClO_4$, pH = 2, T = 20 °C, scan rate 50 mV/s.

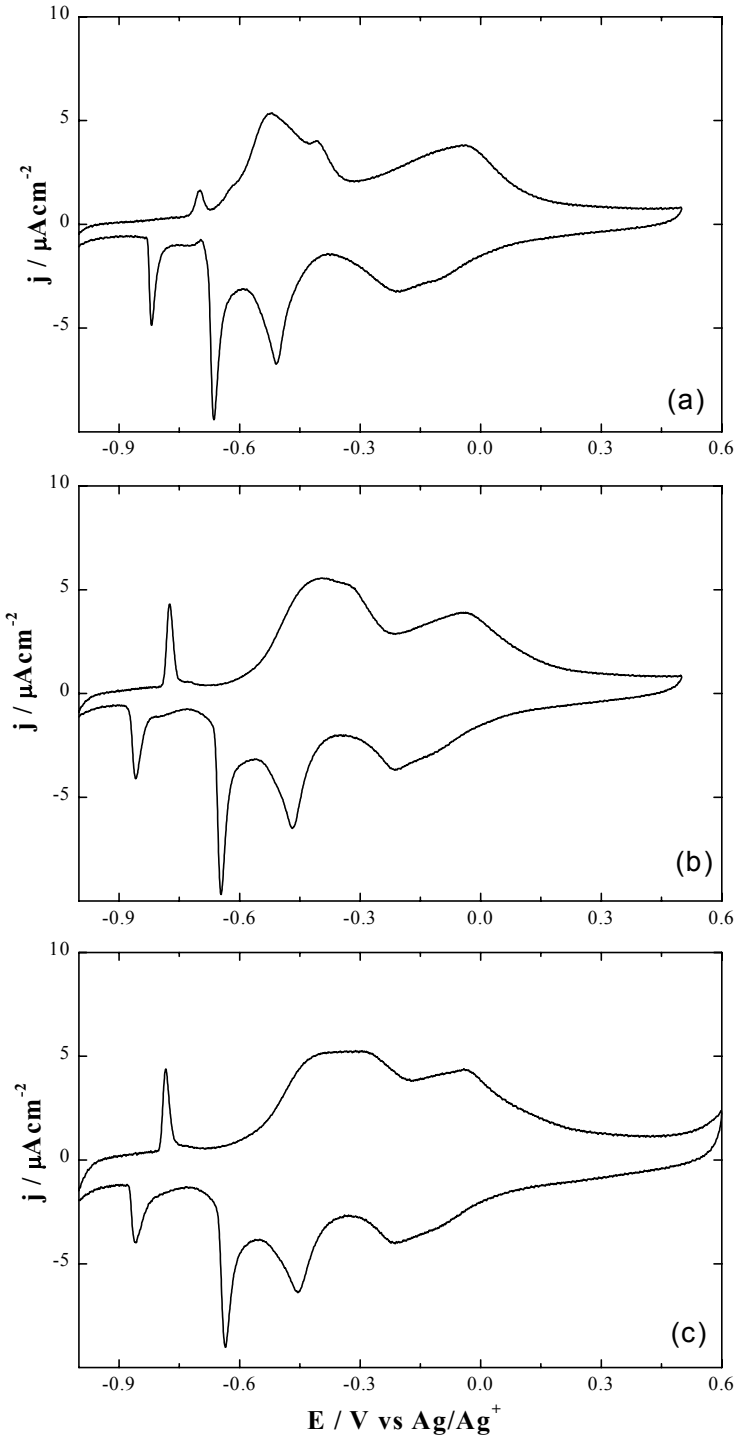


**Figure 4.30:** Cyclic voltammogram of thymine 20 mM + adenine 0.4 mM (a); thymine 20 mM + adenine 0.08 mM (b); and thymine 20 mM + adenine 0.06 mM (c) in 0.1 M $NaClO_4$, pH = 2, T = 10 °C, scan rate 50 mV/s.

In case of thymine adsorption on Au(111), the reorientation of thymine molecules in the chemisorbed state is accompanied by the lifting of reconstruction. For the case of adenine

one can expect similar affections if the molecules are reoriented at potentials > -0.1 V [14,81]. But in either case the lifting of reconstruction and therefore the change of surface ordering due to it takes place in the double layer region at potentials negative of oxidation/reduction. On the other hand, as long as the anodic final potential is negative of the start of oxidation, the voltammograms remain unchanged during several potential scans. This means that the less ordered surface state due to the change between the reconstructed and the unreconstructed surface state is not responsible for the lack of any peaks in the back scans.

Thus, we conclude that the oxidation/reduction process itself affects the surface structure in that way that the size of the terraces becomes smaller due to the reduction probably influenced by adsorbed thymine and adenine, respectively. At this point, detailed surface sensitive investigations are necessary to prove this speculation.

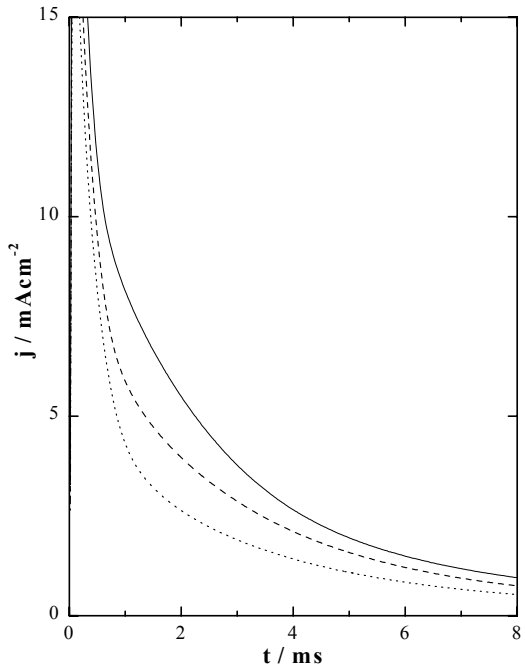


**Figure 4.31:** Current-time transients reflecting the formation of the charge-transfer complex between the π*-orbital of the A-T complex and the d orbitals of the gold surface. Start potential -380 mV to final potentials: (a) –440 mV (solid); (b) –530 mV (dash); (c) –600 mV (dot) for tymine 20 mM + adenine 2 mM in 0.1 M $NaClO_4$, pH = 2, T = 20 °C. Equilibration time: 1 s.

### 4.4.1 DISCUSSIONS

Adenine is adsorbed stronger than thymine, which is proved by comparing the adsorption behavior at different concentration ratios of both bases (Figure 4.24). For concentration ratios adenine/thymine greater than or equal to 0.2 (pH = 2) the obtained CV is identical with that for a pure adenine solution. For smaller ratios the broad chemisorption peak pairs of adenine $A_1/A'_1$ and $A_2/A'_2$ changed their shapes and one can clearly distinguish between two well resolved sharp peak pairs $AT_1/AT'_1$ and $AT_2/AT'_2$. It should be pointed out that the ratio of both bases is more responsible for the shape of the peaks than the absolute concentration of one of the bases at the surface. Narrowing the peak pairs $A_1/A'_1$ and $A_2/A'_2$ at a defined thymine concentration may be taken as a kinetic effect caused by the interaction of adenine with thymine molecules, which leads to a faster kinetics of the adenine/Au charge-transfer complex formation. In contrast to the coadsorption behavior of adenine and thymine on mercury electrodes, where both bases are physisorbed without mutual interaction [31], obviously at the Au(111) electrode both bases interact in the negative potential region. STM investigations [71] show that physisorbed thymine molecules are lying flat in this potential region. The SERS experiments for the adenine molecules reveal a parallel orientation with the plane of the aromatic rings towards the electrode surface [81]. Both bases are therefore oriented in a preferable position to form hydrogen bonds.

At higher pH values the adenine/thymine ratio must be decreased to obtain this kinetic effect on $A_1/A'_1$ and $A_2/A'_2$. This can be explained if one remembers that the adsorption behavior of physisorbed thymine is not influenced in the pH range between 2 and 6 [96], but, on the other hand, the charge-transfer complex formation of adenine is shifted to more negative potentials with an increasing pH value (Figure 4.25) at which the surface concentration of thymine is lowered. For this reason the bulk concentration of thymine must be increased to obtain the necessary critical concentration ratio adenine/thymine at the surface.

For the mechanism of the adenine/thymine complex formation at gold we assume that the peak pairs $AT_1/AT'_1$ and $AT_2/AT'_2$ point to two different surface layers. It is well known that adenine can form different homo dimmers [97]. Three different structures of these dimmers are shown in Figure 4.32.

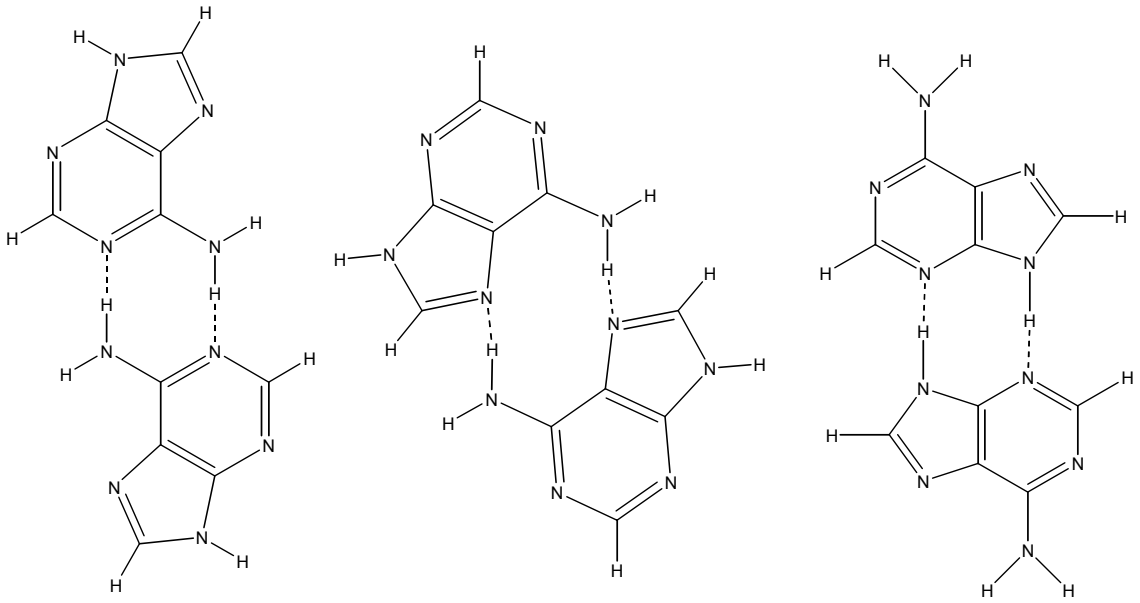

Model A Model B Model C

**Figure 4.32:** Three possible hydrogen-bonding adenine dimmers according to ref. [92].

On graphite surface, structure C is favored for forming a monolayer [98]. However, it cannot be excluded that under electrochemical conditions dimmers with other structures (A and B, respectively) are able to establish adsorbed layers. In X-ray measurements structure B was observed in crystals. It seems to be stabilized by protonation [99]. At this point it is not possible to decide definitely whether different dimmers form differently adsorbed layers or not. It is also not clear how the thymine molecules interact with adenine. But is well seen that in all dimmers exits sites able to form additionally hydrogen bonds.

The kinetics of the formation of the Au-adenine/thymine charge transfer complex is not clear and we refrain from a discussion, particularly because the starting conditions for potential-step experiments are not well defined and several overlapping steps contribute to the kinetics. The measured current-time transients (Figure 4.31) do not follow a pure exponential decay; this does neither a fit pure adsorption nor a first-order phase transition.

The condensed physisorbed layer of thymine indicated by the needle peak pair $T_1/T'_1$could not be found at adenine/thymine ratios greater than 0.02 (T = 20 $^{o}$C, Figure 4.24

and Figure 4.26). At a first glance, it seems that this is in accordance with the results found for the coadsorption behavior of adenine and thymine on mercury. But one should not forget that adenine adsorbs much more stronger at Au(111) than thymine. At potentials negative of the peak pairs $AT_1/AT'_1$ and $AT_2/AT'_2$ the adenine/thymine charge transfer complex is adsorbed. The strong adsorption of adenine and its interaction with thymine indirectly lead to immobilization of thymine. The concentration of thymine molecules being mobile at the surface is therefore considerably decreased. Obviously, at ratios adenine/thymine larger than 0.02 the critical concentration of mobile thymine molecules necessary for the formation of the condensed thymine layer is not reached. Most of the thymine molecules at the surface are "prisoners" of the immobilized adenine molecules.

At small adenine/thymine ratios (0.004 for 20 $^{o}$C, Figures 4.26 and 4.28, and 0.2 for 10 $^{o}$C, Figure 4.30) sufficient "mobile" thymine molecules are present to form an ordered physisorbed thymine phase. This occurs at potentials negative of the peak pairs $AT_1/AT'_1$ and $AT_2/AT'_2$. The temperature behavior of $T_1/T'_1$ is therefore in accordance with the temperature behavior of pure condensed thymine monolayers [71]. In the potential region between the needle peak pair $T_1/T'_1$ and the peak pairs $AT_1/AT'_1$ and $AT_2/AT'_2$ the appearance of domains of ordered physisorbed thymine besides domains consisting of the Au-adenine/thymine charge transfer complex may be assumed. Even if the $AT_1/AT'_1$ and $AT_2/AT'_2$ peak pairs are too small to be detected at very low adenine/thymine concentration ratios (smaller than 0.0004 up to 0.00005, Figures 4.28 and 4.29), the adsorbed adenine influences the physisorbed condensed thymine, i.e., the peak position $T_1/T'_1$ is shifted to more positive potentials in comparison to that for a pure thymine solution.

Although at potentials positive of the peak pairs $AT_1/AT'_1$ and $AT_2/AT'_2$ (Figure 4.24) adenine is not chemisorbed, it is so strongly adsorbed even in its physisorption state that it prevents a well defined and complete formation of the chemisorbed thymine layer. The broad wave $T_{2/3}/T'_{2/3}$ indicates that only a small amount of thymine is adsorbed.

The positive shift of the peak pairs $AT_1/AT'_1$ and $AT_2/AT'_2$ at adenine/thymine ratios smaller than 0.004 (Figures 4.26, 4.28 and 4.30) shows that an increase of the relative surface concentration of thymine favors the formation of the charge transfer complex between the lowest unoccupied $\pi^*$-orbital of adenine and the highest occupied d-orbital of Au(111). This means that the energy of the $\pi^*$-orbital is lowered by the interaction between thymine and adenine. Guerra *et al.* [100] have shown that the formation of hydrogen bonds between adenine and thymine leads to an increase of negative charge on thymine due to the different

interactions between the involved π-orbitals. Although the π-electron density is not involved in the formation of hydrogen bonds, the π-system is influenced by the electrostatic potential, which both bases experience from each other. The π-system wants to eliminate the charge differentiation by the π-hydrogen bonds and becomes polarized, or, in other words, the energy of the π-orbital increases. Consequently, the energy of the π*-orbital decreases. The charge- transfer complex formation between gold and adenine is therefore energetically favored; the more hydrogen bonds between adenine and thymine are formed.

The broad signals $T_{2/3}/T'_{2/3}$ are correlated with the formation and dissolution of the chemisorbed thymine phase. With decreasing adenine concentration this peak pair splits into separated signals, as found for pure thymine solution.

The coadsorption behavior of A-T at polycrystalline electrode produces very different cyclic voltammograms when compared with the coadsorption on Au(111) electrode. On a polycrystalline surface, the CV's do not shows any well defined peaks, only broad waves around –0.15 V and -.050 V are obtained respectively (Figure 4.33). In the capacity curves different adsorption regions can be recognized. Two minima are well-resolved, broad one at negative potentials and a smaller one at positive potentials. Comparing with the results on Au(111) we interpret the minimum at negative potentials corresponding to the A-T charge transfer complex. Consequently, this minima shift to more positive potentials with smaller adenine concentration (Figure 4.34). The small minimum at the positive potential show us the presence of both molecules adenine and thymine at the surface, but nevertheless not so strong adsorbed as the A-T charge transfer complex at the negative potential region.

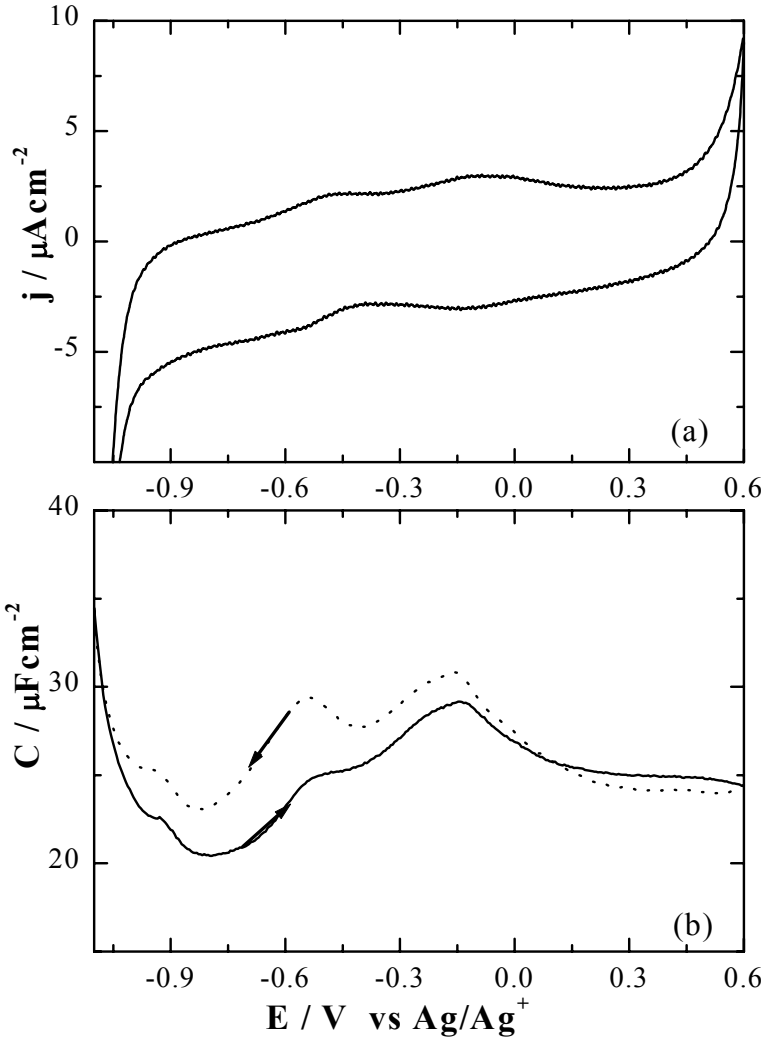


**Figure 4.33:** Cyclic voltammogram of thymine 20 mM + adenine 3 mM on Au polycrystalline in 0.1 M $NaClO_4$, T = 20 °C, scan rate 50 mV/s (a) and capacity curves, F = 20 Hz (b).

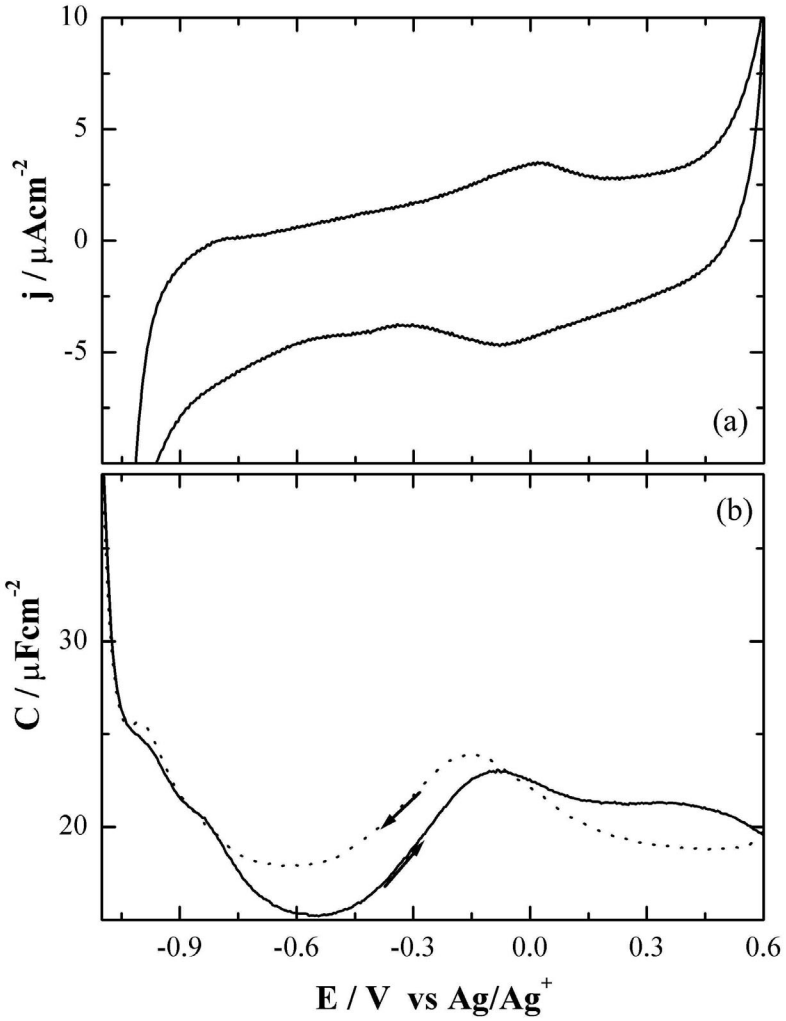


**Figure 4.34:** Cyclic voltammogram of thymine 20 mM + adenine 0.08 mM on Au polycrystalline in 0.1 M $NaClO_4$, T = 20 °C, scan rate 50 mV/s (a) and capacity curves, F = 20 Hz (b).

## 4.5 COADSORPTION OF THYMINE AND URACIL ON AU(111)

Similar as the complementary base pairs adenine-thymine, thymine can form hydrogen bond with uracil. The questions that should be answered are: does interact thymine with uracil on the electrode surface? Is the interaction comparable with the interaction between the complementary base pairs?

It is known that uracil form at negative potentials a physisorbed condensed film, whereby uracil is similar as thymine and adenine is planar orientated at the electrode surface

(Figure 4.35). Due to the similar adsorption behavior of uracil and thymine, the experiments start with a mixture thymine /uracil 5 mM / 6 mM at pH = 2.

The resulting cyclic voltammogram for the mixture at the same concentration of uracil and thymine is shown in Figure 4.36. The phase-transition peaks for thymine ($T_1/T'_1$) can be clearly detected, but at lower intensity and shifted to more positive potentials compared with that for pure thymine. Comparing the position of these needle peaks with the same peak pairs for the single bases (Figure 4.35), it is seems that the formation of the physisorbed thymine layer is influenced by the adsorbed uracil molecules in such way that the critical nucleation concentration for the formation for the first nucleous is reached at more positive potentials. The peaks denoted for the transformation into the chemisorbed state look more like the peaks $U_2/U_3$ $U'_2/U'_3$ (Figure 4.35 (a)) for uracil than that for thymine (Figure 4.35 (b)). It seems that uracil molecules mostly influence the transition into the chemisorbed state. So it can be concluded that thymine and uracil form the condensed film together.

The effect become more evident by lowering the concentration ratio of uracil / thymine (Figure 4.37). At an uracil concentration of 3 mM (uracil / thymine ratio 3 mM / 5 mM) (Figure 4.37 (a)) the needle peaks ($T_1/T'_1$) shift into more negative direction and for an uracil concentration of 1 mM at constant thymine concentration (5 mM) the peaks $T_1/T'_1$ become more pronounced than for the concentration ratio before (Figure 4.37 (b)). The shape of the peaks denoted for the transformation into the chemisorption region becomes closest to that for thymine the lower the uracil concentration is.

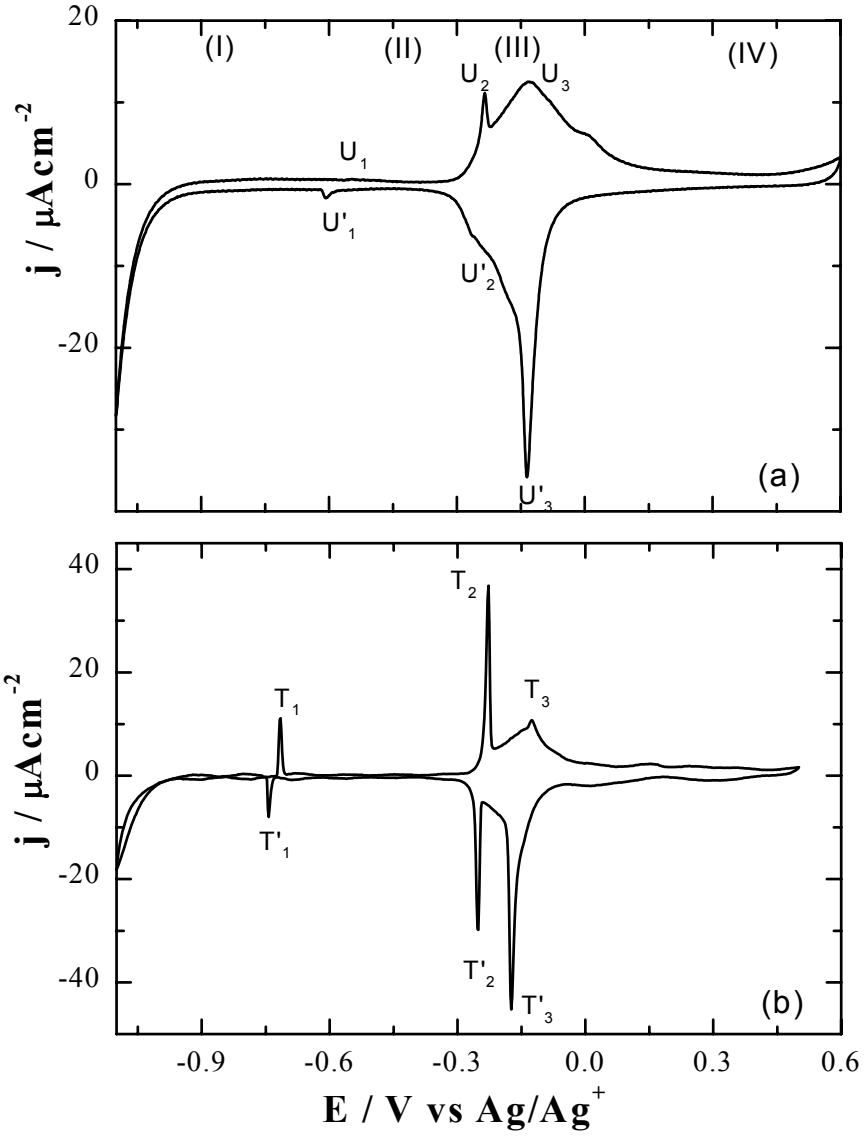


**Figure 4.35:** Cyclic voltammograms of 6 mM uracil (a) and 5 mM thymine (b) in 0.1 M $NaClO_4$, pH = 2, T = 20 °C, scan rate 50 mV/s. $U_1/U'_1$and $U_2/U'_2$: formation and dissolution of the charge-transfer complex between uracil and the gold surface; $T_1/T'_1$: formation and dissolution of the ordered physisorbed thymine monolayer; $T_2/T'_2$ dissolution and formation of the ordered physisorbed thymine monolayer; $T_3/T'_3$ formation and dissolution of the ordered chemisorbed thymine monolayer;

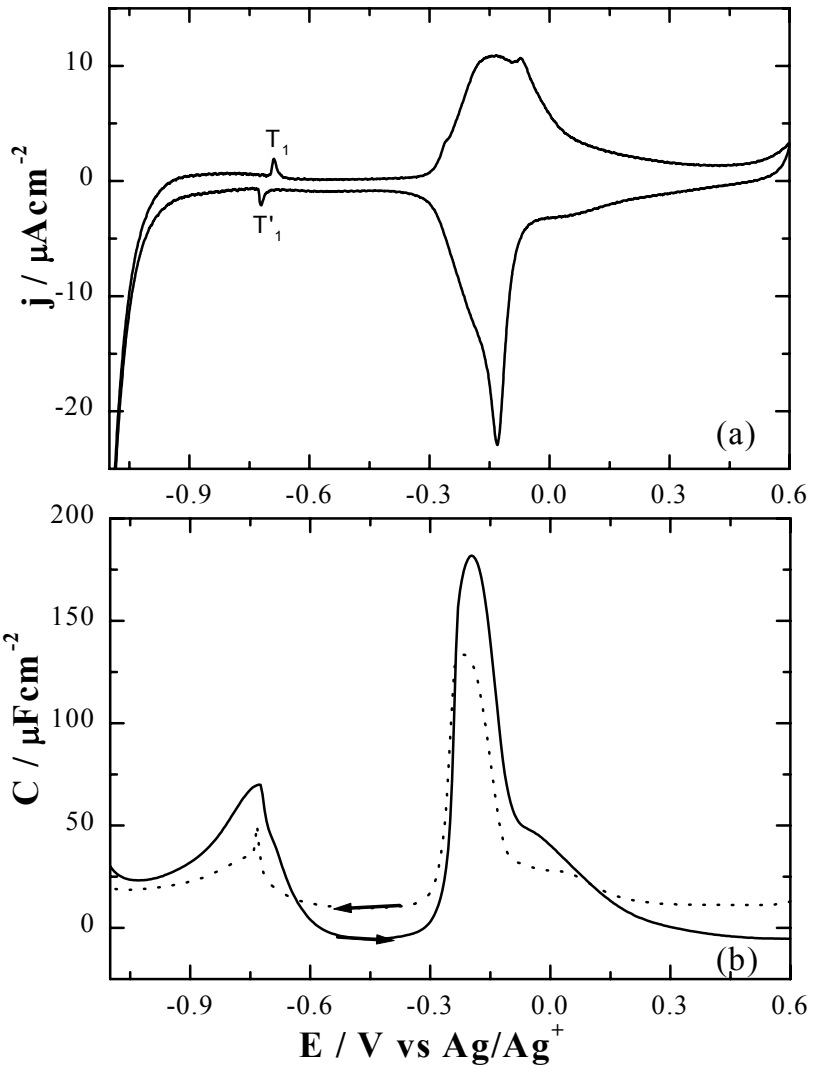


**Figure 4.36:** Cyclic voltammogram of thymine 5 mM + uracil 6 mM (a) and capacity curves (b) in 0.1 M $NaClO_4$, pH = 2, T = 20 °C, scan rate 50 mV/s, F = 20 Hz.

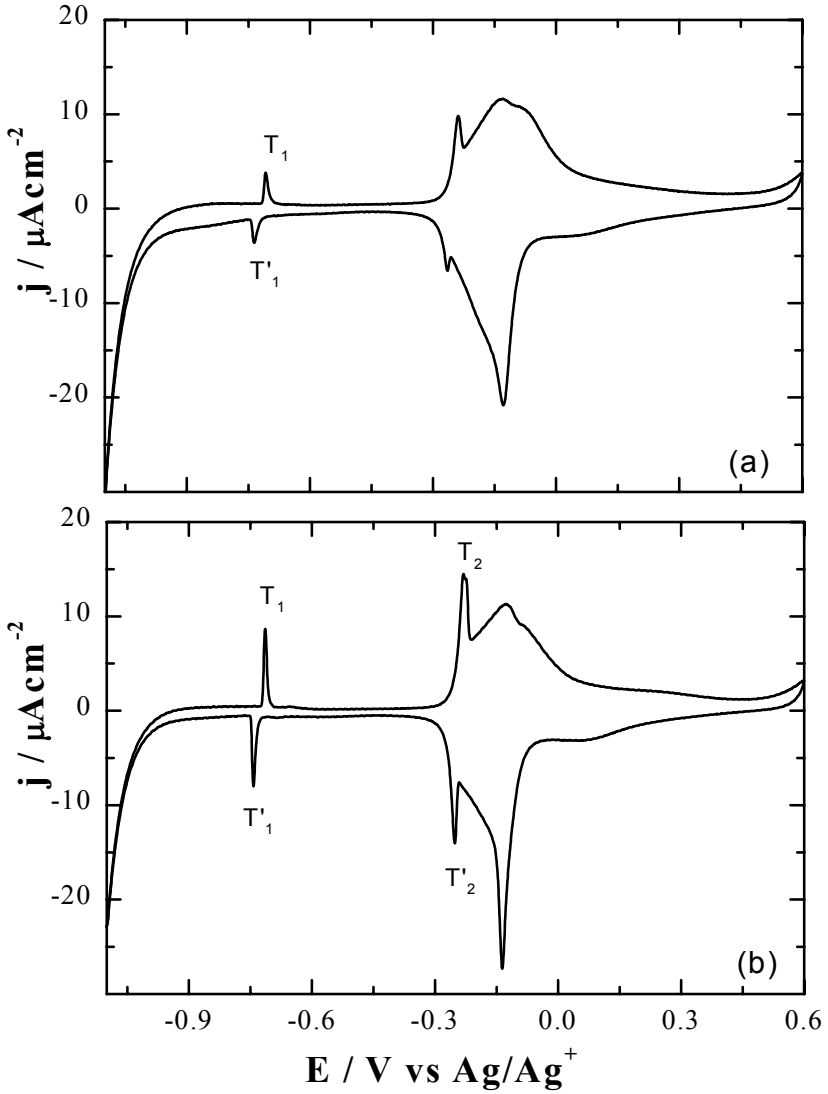


**Figure 4.37:** Cyclic voltammogram of thymine 5 mM + uracil 3 mM (a); thymine 5 mM + uracil 1 mM in 0.1 M $NaClO_4$, pH = 2, T = 20 °C, scan rate 50 mV/s.

A small thymine concentration (1 mM) prevents the formation of physisorbed film of uracil (6 mM), according to the result shown in Figure 4.11. The small concentration of thymine is not sufficient to provide the critical nucleation concentration of the surface necessary to form thymine nucleous. Otherwise the lowering of the effective uracil concentration hindered kinetically the formation of a critical uracil nucleous. The formation of the chemisorbed phase is mostly determined by the formation of the uracil molecules. It is possible that the faster transformation kinetics of uracil overlap the transformation of thymine molecules.

Increasing the thymine concentration (2 mM) and decreasing the uracil concentration (3 mM) leads to the same CV as before (Figure 4.38 (b)), i.e., the electrode surface is covered mostly by the uracil molecules.

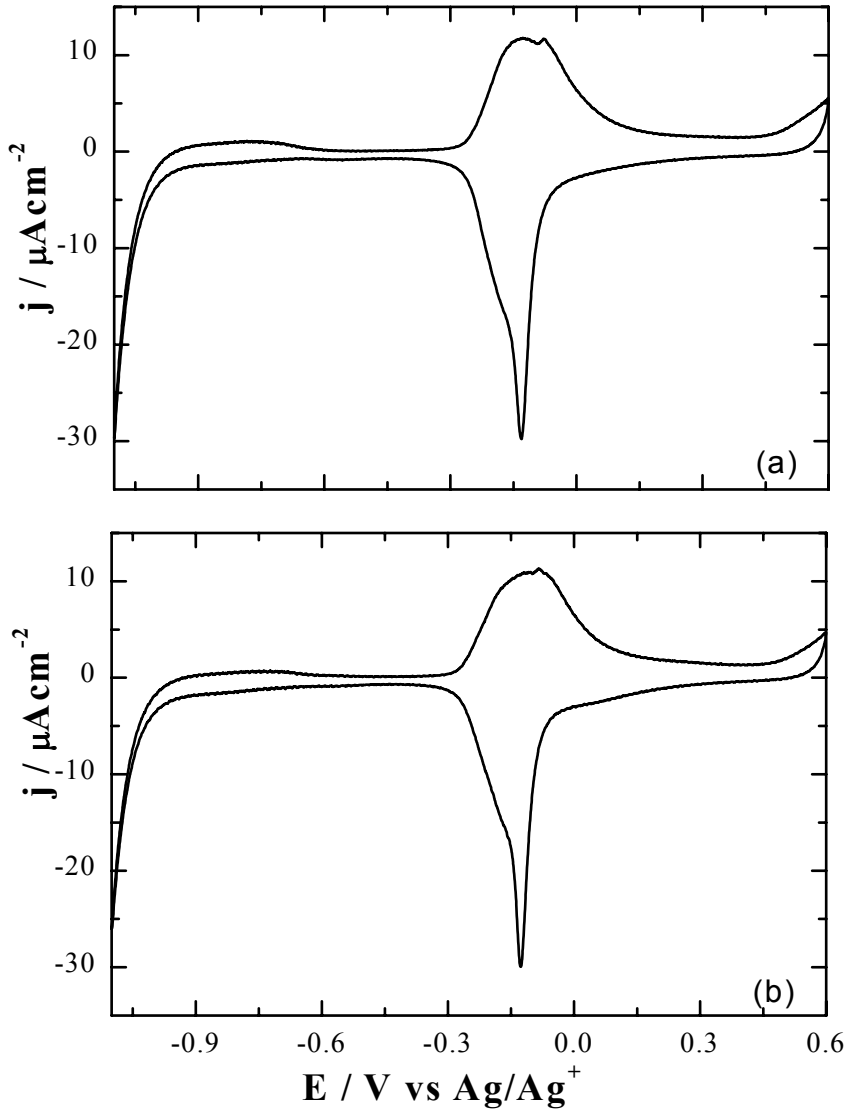


**Figure 4.38:** Cyclic voltammogram of thymine 1 mM + uracil 6 mM (a); thymine 2 mM + uracil 3 mM (b) in 0.1M $NaClO_4$, pH = 2, T = 20 °C, scan rate 50 mV/s.

## 4.6 SUMMARY

Adenine is strongly adsorbed at Au(111) in the double layer region. No first-order phase transitions like those of thymine/Au(111) were observed, but two different states of chemisorbed adenine are evident.

At negative potentials the plane of adenine is oriented parallel to the electrode surface. This geometry allows a partial charge transfer from the electrode surface to the □-system of the heteroaromatic molecule.

A second chemisorbed adsorbate of adenine exists at more positive potentials. In this potential range also thymine is chemisorbed. The plane of the chemisorbed thymine is oriented perpendicular to the electrode surface. In analogy, we assume this orientation for adenine in this potential range. We found no experimental features pointing to a mutual interaction of adenine and thymine in this orientation.

In mixtures of adenine and thymine, the shape of the signals assigned to adenine chemisorption is strongly influenced by thymine. This reveals an attractive interaction of adenine and thymine in this adsorbate. By this interaction the formation of the thymine condensed layer is blocked at a value above a critical adenine/thymine concentration ratio.

Thymine adsorbs stronger than uracil and prevents the uracil phase-transition. On the other hand, uracil hinders the formation of the condensed monolayer consisting of thymine alone, which is seen by a shift of the corresponding peak pairs $T_1/T'_1$. No mutual interaction could be found.